



INSTITUTO POTOSINO DE INVESTIGACIÓN  
CIENTÍFICA Y TECNOLÓGICA, A.C.

POSGRADO EN CIENCIAS APLICADAS

**Interaction between carbon nanotubes and biological  
systems**

Tesis que presenta

Antonio Esaú Del Río Castillo

Para obtener el grado de

Maestro en Ciencias Aplicadas

En la opción de

Nanociencias y Nanotecnología

Realizada bajo la codirección de:

Dr. Mauricio Terrones Maldonado

Dra. Ana Paulina Barba De La Rosa

San Luis Potosí, S.L.P., México, septiembre de 2008

# Interaction between carbon nanotubes and biological systems

Antonio Esaú Del Río Castillo

Thesis presented for the degree of  
Master in Applied Sciences,  
Option in Nanosciences and Nanotechnology

Co-supervised by:

Dr. Mauricio Terrones Maldonado

Dr. Ana Paulina Barba De La Rosa



Advanced Material Division  
Potosian Institute of Technology (IPICYT)  
San Luis Potosí, S.L.P., México  
September 2006



## Constancia de aprobación de la tesis

La tesis "Interaction between carbon nanotubes and biological systems" presentada para obtener el Grado de de Maestro en Ciencias Aplicadas en la opción de Nanociencias y Nanotecnología fue elaborada por **Antonio Esau Del Rio Castillo** y aprobada el 28 de Agosto de 2008 por los suscritos, designados por el Colegio de Profesores de la División de Materiales Avanzados del Instituto Potosino de Investigación Científica y Tecnológica, A.C.

---

Dr. Mauricio Terrones Maldonado  
Co-Director de la tesis

---

Ana Paulina Barba de La Rosa  
Co-Director de la tesis

---

Dra. Yodha Vega Cantú  
Miembro de comité



## **Créditos Institucionales**

Esta tesis fue elaborada en el Laboratorio de Nanoestructuras de la División de Materiales Avanzados para la Tecnología Moderna del Instituto Potosino de Investigación Científica y Tecnológica, A.C., bajo la codirección del Dr. Mauricio Terrones Maldonado y la Dra. Ana Paulina Barba Da La Rosa.

Durante la realización del trabajo el autor recibió una beca académica del Consejo Nacional de Ciencia y Tecnología y del Instituto Potosino de Investigación Científica y Tecnológica, A. C.



**IPICYT**

# Instituto Potosino de Investigación Científica y Tecnológica, A.C.

## Acta de Examen de Grado

El Secretario Académico del Instituto Potosino de Investigación Científica y Tecnológica, A.C., certifica que en el Acta 020 del Libro Primero de Actas de Exámenes de Grado del Programa de Maestría en Ciencias Aplicadas en la opción de Nanociencias y Nanotecnología está asentado lo siguiente:

En la ciudad de San Luis Potosí a los 11 días del mes de septiembre del año 2008, se reunió a las 09:00 horas en las instalaciones del Instituto Potosino de Investigación Científica y Tecnológica, A.C., el Jurado integrado por:

<b>Dr. Mauricio Terrones Maldonado</b>	<b>Presidente</b>	<b>IPICYT</b>
<b>Dr. Roberto González Amaro</b>	<b>Secretario</b>	<b>UASLP</b>
<b>Dra. Ana Paulina Barba De la Rosa</b>	<b>Sinodal</b>	<b>IPICYT</b>
<b>Dra. Yadira Itzel Vega Cantú</b>	<b>Sinodal</b>	<b>IPICYT</b>

a fin de efectuar el examen, que para obtener el Grado de:

### MAESTRO EN CIENCIAS APLICADAS EN LA OPCIÓN DE NANOCIENCIAS Y NANOTECNOLOGÍA

sustentó el C.

**Antonio Esaú del Río Castillo**

sobre la Tesis intitulada:

#### *Interaction between carbon nanotubes and biological systems*

que se desarrolló bajo la dirección de

**Dra. Ana Paulina Barba De la Rosa**  
**Dr. Mauricio Terrones Maldonado**

El Jurado, después de deliberar, determinó

**APROBARLO**

Dándose por terminado el acto a las 11:10 horas, procediendo a la firma del Acta los integrantes del Jurado. Dando fe el Secretario Académico del Instituto.

A petición del interesado y para los fines que al mismo convengan, se extiende el presente documento en la ciudad de San Luis Potosí, S.L.P., México, a los 11 días del mes de septiembre de 2008.

**L.C.C. Juan Carlos Cuervo Velez**  
Jefe del Departamento de Asuntos Escolares

*Mauricio Terrones Maldonado*  
**Dr. Mauricio Terrones Maldonado**  
Secretario Académico



## *Dediacada a*

Mi familia y amigos, quienes siempre me han dado su apoyo.

## AGRADECIMIENTOS

Quisiera agradecer a mis asesores, la Doctora Ana Paulina Barba y el Doctor Mauricio Terzanos por compartir conmigo sus conocimientos y siempre brindarme su apoyo durante el desarrollo de esta tesis. Del mismo modo a la Doctora Yadira Vega por sus valiosos comentarios y sugerencias para esta tesis. Al Doctor Roberto González por aceptar ser mi asesor externo.

También al personal técnico que siempre están al pendiente y siempre a prestar su apoyo, Grises Ramírez, Daniel Ramírez, Gabriel Oedóñez, Hugo Martínez, Ferdinando Tristán, Magdalena, Dulce Partida y Alberto Barrera. A Víctor Mata. También agradezco a Haydee Portillo (UASLP) por su apoyo en la caracterización, al Doctor J. P. Shields (Georgia University) por sus consejos en la preparación de muestras biológicas David Kicoyne (Berkeley Univ.) por su apoyo en caracterización de muestras, y a Lourdes Palma (CNAM, Juicquilla) por su gran ayuda aconsejándome y apoyo para el corte en ultramicrotomo. También agradezco el invaluable apoyo del personal administrativo Ivonne Cuevas, Edith Rodríguez, Gaby Pérez y Karla Gómez, a Don Raúl a Adella.

Estoy también muy agradecido con los profesores que me han compartido un poco de sus vastos conocimientos durante mi estancia en el IPICYT, al Dr. Humberto Terzanos, al Dr. Fernando Rodríguez, al Dr. Haot Ren, al Dr. Emilio Muñoz, al Dr. Florentino López, al Dr. Román Sandoval, la Dra. Elizabeth Hubert, al Dr. Antonio de León, al Dr. Daniel Hernández, al Dr. J. Luis R. y especialmente a la recién Doctora Fabiola Galván por su increíble apoyo al desarrollo de esta tesis.

A mi compañera del IPICYT con los cuales siempre me apoyaron durante mi estancia Alberto Zamudio, Ana Laura Illías, Eduardo Cruz, Jaime Pérez, Pily Moonivas, Pedro Palomares, Vianey Bojórquez, Xavier Lepro, Claudia Guadalupe, Abraham Cano, Andrés Borello, Eduardo Gracia Jessica Campos, Samuel Baltasar, Aaron Morelos, Rodrigo Rentaría, Erika Briones, Hugo Aguilar, Luis Martínez, Berenice Ortega, Aurora, Enrique Maldonado y Julia Acosta.

Quiero agradecer especialmente a Edith Isela Torres por su apoyo incondicional, en todos los aspectos, en estos últimos meses que han sido difíciles, y gracias a ella los he podido superar.

A mis padres, mi hermano, mis abuelitos y viejos amigos, que aunque se encuentran relativamente lejos siempre me apoyaron.

Finalmente a CONACYT por el apoyo económico que me permitió realizar este trabajo.

# Contents

Constancia de aprobación de la tesis	v
Créditos Institucionales	vii
Certificate of degree examination	ix
Dedicatoria	xi
Agradecimientos	xiii
Resumen (Abstract)	xxiii
1 The Cell and Bio-applications of Carbon Nanotubes	2
The cell, a brief review	4
Bacteria	6
Human being, an Eukaryote organism	7
The cell membrane	11
Cellular cycle	14
Cancer Cells	18
Carbon Nanostructures, a brief review	20
Properties of Carbon Nanotubes	21
Synthesis, functionalization and bio-applications of Carbon Nanotubes	25



References	29
2. Multiwalled Carbon Nanotubes, synthesis and characterization	32
Nanotubes Synthesis	34
Functionalization, cleaning and dispersion of Carbon Nanotubes	36
Nanotubes Characterization	38
Scanning electron microscopy and Energy Dispersive X ray analysis	38
Raman Spectroscopy	45
References	48
3. Interactions between Human cells and Multiwalled Carbon Nanotubes	50
Materials and Methods	54
Experimental design	55
Characterization	57
Flow Cytometry-Fluorescence activated cell sorting	57
Scanning-Transmission Electron microscopy	60
Results & Discussion	63
Flow Cytometry-Fluorescence activated cell sorting	63
Scanning-Transmission Electron microscopy	71
References	82
4. Interactions between <i>Bifidobacterium longum</i> and Multiwalled Carbon Nanotubes	86
Materials and Methods	90
Experimental Design	92
Characterization	94
Results and Discussion	95

References	108
5. Conclusions and future work	112
Conclusions	113
Future work	115
Appendix A Cell Culture maintenance.	116
Appendix B Flow cytometry, nucleus staining for FACS	117
Appendix C. Cell preparation for Electron microscopy. Scanning and Transmission electron microscopy	118
Appendix D Bacteria Transformation	124
Electroporation	124
Heat shock	125
Microwave	125
Appendix E. MRS Medium preparation	126

# List of figures

1.1	Organization of Prokaryote and Eukaryotic	5
1.2	Gram positive and negative membranes	7
1.3	Eukaryote cell	9
1.4	Lipid composition of bilayer membrane	12
1.5	Model of membrane structure	13
1.6	Stages of Eukaryotic cells	15
1.7	Successive phases in mitosis of yeast	16
1.8	Comparison between healthy and Apoptotic cells	17
1.9	Classification of Carbon Nanotubes	22
1.10	Density of States of Zigzag and armchair nanotubes	23
1.11	Density of states of Nitrogen doped nanotubes	24
1.12	Non-covalent molecules attached to nanotubes	26
1.13	Importance on rate volume-area in nanomaterials	28
2.1	Nanotubes dispersability probes in different solvents	37
2.2	CNTs dispersed in water	42
2.3	CNTs dispersed in cell culture medium	42
2.4	Raman Spectra of oxidated MWNTs	47
3.1	Flow cytometer system	57
3.2	Typical Flow Cytometry pattern	60
3.3	Embedded cells into epoxy resin	62
3.4	Plot of percentage of apoptotic HEK cells treated with different CNTs	64

3.5	Plot of percentage of apoptotic HEK cells treated with different CNTs, with a concentration of $5\mu\text{g ml}^{-1}$	65
3.6	Plot of cell cycle and percentage of apoptotic HeLa cells when are treated with different types of CNTs	67
3.7	Plot of cell cycle and percentage of apoptotic CaSki cells when are treated with different types of CNTs	70
3.8	HEK cell	71
3.9	HEK cell treated with functionalized CNx-MWNTs	72
3.10	f-CNx-MWNT deforming membrane of HeLa cell	73
3.11	HEK cell treated with functionalized COx-MWNTs	74
3.12	HeLa cell without treatment	75
3.13	HeLa cell treated with functionalized COx-MWNT	76
3.14	HeLa cell treated with functionalized MWNT	77
3.15	CaSki cell in mitosis	78
3.16	CaSki cell treated with functionalized COx-MWNT	79
3.17	CaSki cell treated with functionalized CNx-MWNT	80
3.18	CaSki cell treated with functionalized MWNT	81
4.1	pRI plasmid	91
4.2	Time versus temperature diagram for PCR	95
4.3	Statistic curves for Nanotubes length distribution	96
4.4	MRS-Agar plate with <i>Bifidobacterium longum</i> culture	97
4.5	PCR amplification for different colonies transformed	99
4.6	<i>Bifidobacterium longum</i> after cell division	100
4.7	<i>Bifidobacterium longum</i> treated with small diameter CNTs	101
4.8	CNTs pinned into <i>Bifidobacterium longum</i> membrane	102
4.9	Big diameter CNTs as templates for <i>Bifidobacterium longum</i>	103
4.10	Big Bacteria	104

4.11	60 nm thick fCNx-MWNT pinned into bacteria	105
4.12	STEM image of <i>B. longum</i> and fCNx-MWNT	106
4.13	STEM sequence images of <i>B. longum</i> and fCNx-MWNT	107

# List of tables

1.1	Prokaryote and eukaryote cells	6
1.2	Cell adhesion molecules	14
1.3	Carbon isomers	21
2.1	Elemental analysis, EDX for pristine MWNTs	39
2.2	Elemental analysis, EDX for pristine CN <sub>x</sub> -MWNTs	39
2.3	Elemental analysis, EDX for pristine CO <sub>x</sub> -MWNTs	39
2.4	Elemental analysis, EDX for MWNTs after 2 hours of acid treatment	40
2.5	Elemental analysis, EDX for CN <sub>x</sub> -MWNTs after 2 hours of acid treatment	40
2.6	Elemental analysis, EDX for CO <sub>x</sub> -MWNTs after 2 hours of acid treatment	40
2.7	Overview of results from EDX characterization	41
2.8	Relative intensities $I_D/I_G$ , $I_2/I_2'$ and $I_D/I_2'$ of Raman peaks for pristine and oxidized CNTs	47
3.1	Treatments made to HeLa, CaSki and HEK cells with three types of CNTs	56
3.2	Percentage of apoptotic HEK cells treated with CNTs	62
3.3	Percentages of HeLa cells in different phases of cell cycle when are treated with three different CNTs at different doses	66
3.4	Percentages of CaSki cells in different phases of cell cycle when are treated with three different CNTs at different doses	69

4.1	Transformation rate of <i>B. lonum</i> with three different transformation methods and CNTs.	97
4.2	Transformation rate reported for three different groups, all were made by electroporation and used high voltages	98

# Interaction between carbon nanotubes and biological systems

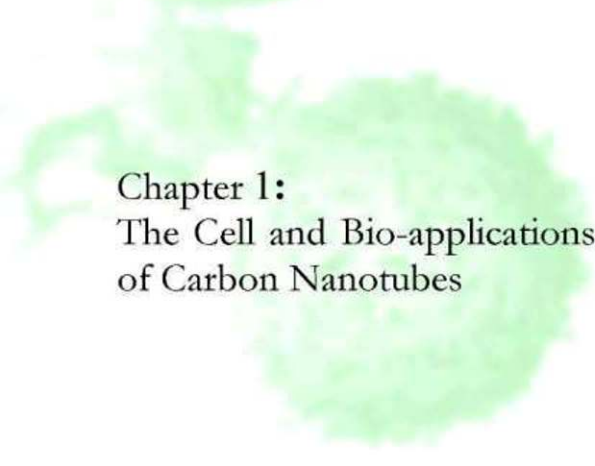

Antonio Esaú Del Río Castillo

Submitted for the degree of Master in Applied Sciences  
September 2008

## Abstract

It is well known that carbon nanotubes (CNTs) have outstanding physical and chemical properties, and these properties could be modified by doping, adding defects or by functionalizing the surface of the tubes. When CNTs interact with biological molecules, the dispersability and hydrophobicity are important parameters. In this work, we studied the interaction of human cells (HeLa, CaSki and HEK) with different types of nanotubes: a) pure carbon multi-walled CNTs (MWNTs), b) N-doped multi-walled CNTs (CNx-MWNTs), and functionalized multi-walled CNTs (COx-MWNTs). We studied the cell changes in their cycles, and how the apoptotic rate is altered, depending on the nanotube type and concentration in solutions. The possibility of using carbon nanotubes for oncological treatments will also be discussed. In addition, we propose the use of different types of CNTs for genetic transformations in bacteria. In particular, we were able to enhance the genetic transformation rate by two orders of magnitude for the *Bifidobacterium longum*, when adding CNTs to the traditional transformation protocols. We believe that in the future, carbon nanotubes could help the development of new cancer treatments and the production of efficient drug delivery carriers.





**Chapter 1:**  
The Cell and Bio-applications  
of Carbon Nanotubes

## The cell, a brief review.

The fundamental life unit is the cell; it is the smallest form of life and fulfills all the requirements of a living system. Inside a number of chemical reactions occur allowing the growth, reproduction, information processing, stimuli, etc. These abilities defines the life, thus, even simple unicellular organisms exhibit all the properties of life.

Cells are categorized in two main groups depending whether they contain nucleus or not: **Prokaryotes** which are that lack of a defined nucleus, and consist of single compartment surrounded by plasma membrane, and exhibit relatively simple internal organization (see Figure 1.1 a). Bacteria are the most numerous prokaryotes, and are divided in two groups: archaebacteria, which can live under extreme environments; and eubacteria, consisting of large group of organisms capable of living in a wide range of environments. **Eukaryotic** cells displays a well defined nucleus, which contains the genetic

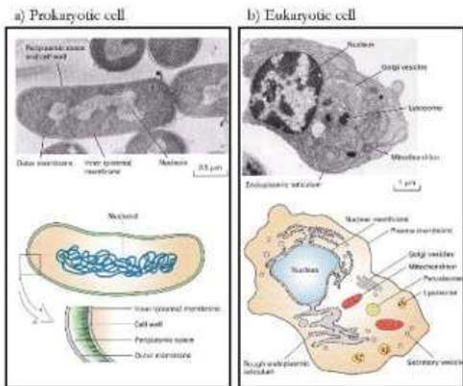


**Figure 1.1:** Organization of Prokaryotic and Eukaryotic cells. a) Electron micrograph of a thin section of *Escherichia coli*, the nucleoid, consisting of bacterial DNA, is not enclosed by a membrane. The thin cell wall is adjacent to the inner membrane. b) Electron micrograph of a plasma cell. Only a single membrane surrounds the cell, but the interior contains several membrane limited organelles. Image taken from [1] [2]

information of the cell, as well as extensive internal membrane that enclose other complex organelles (see Figure 1.1 b). Eukaryotic cells are generally larger than prokaryotic cells, which frequently exhibit a volume at least thousand times greater.

Human cells are eukaryotic cells. Animals, plants, fungi and protists are eukaryotic cells too. All these variations come from one ancestral cell, even prokaryotes probably come from an older ancestral common cell.

**Table 1.1:** Prokaryotic and Eukaryotic Cells (Take from [3])

Characteristic	Prokaryote	Eukaryote
Nucleus	Absent	Present
Diameter	~1 $\mu$ m	10-100 $\mu$ m
Cytoskeleton	Absent	Present
Cytoplasmic organelles	Absent	Present
DNA content (base pairs)	1x10 <sup>7</sup> to 5x10 <sup>8</sup>	1.5x10 <sup>9</sup> to 5x10 <sup>9</sup>
Chromosomes	Single circular DNA molecule	Multiple linear DNA molecules

## Bacteria

Bacteria are Prokaryote (unicellular organisms) and are the simplest form of life because they do not have organelles; their genetic material is dispersed in cytosol without internal membranes enclosing it, additional DNA is found in a circular shape named plasmid. It is important to say that not all bacterial have plasmid DNA.

Bacteria are present in every habitat on Earth, from soil to the Earth's crust, passing trough acidic hot springs, radioactive waste [4], and deep and hot seawater. Interestingly, bacteria are ten times more numerous in the human body than human cells. The number of bacteria on Earth is ca. 5x10<sup>30</sup> [5], thus these small organisms constitutes a fundamental issue for life.

There are two types of bacteria which are classified as Gram positive or negative depending on membrane characteristics. Gram positive bacteria contain a single plasma membrane surrounded by a thicker cell wall, this cell wall determines shape and protect cell against osmotic and thermal damages. Gram negative bacteria exhibit a dual membrane, and the plasma membrane is surrounded by a very thin cell wall sandwiched by an outer membrane. Figure 1.2 illustrates the differences between these two categories.

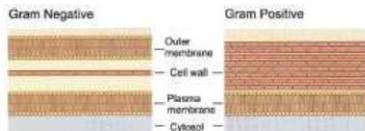


**Figure 1.2** Schematic diagram showing the differences between Gram positive and Gram negative membrane cells.

Some types of Gram positive bacteria are *Bifidobacterium*, *Bacillus*, *Listeria*, *Staphylococcus*, *Streptococcus*, *Enterococcus*, and *Clostridium*. Genus of Gram negative bacteria are *Proteobacteria* (like *E. coli*), *Enterobacteriaceae*, *Pseudomonas*, *Moraxella*, *Helicobacter*, *Sinetrophomonas*, etc.

## The Human being as an eukaryote organism

In 1827 Karl von Baer discovered that mammals grow from eggs that come from the mother's ovary. Fertilization of an egg by a sperm cell yields a

zygote. Every human being starts developing as a zygote, which process all the necessary information to build the human body containing about one trillion ( $10^{13}$ ) cells. This development begins with the fertilized egg cell dividing in two, four, eight cells, until forming a very early embryo. The continuation of the cell proliferation and the differentiation on to different cell types give rise to every tissue in the human body. One initial cell, the fertilized egg, generates hundreds of different kinds of cells, which differ in content, shape, size, color, mobility, and surface composition [Ref. 2, pag. 7]

In the human body exists almost 210 different cell types, and all of them carry out a unique and special function. For example, blood contains several different types of cells, whose functions are widely varied, some of these cells are responsible for oxygen transport (known as red cells or erythrocytes); others address inflammatory reactions (granulocytes and monocytes) as well as these dealing with the immune response (lymphocytes). Despite all their diverse forms and functions, all animal cells can be classified in five main categories according to their classes of tissues: epithelial, connective, muscular, nervous and blood.

Figure 1.3 depicts an eukaryote cell displaying the main characteristics and organelles in this kind of cell. The principal characteristic of eukaryote cells is the presence of a well defined nucleus which encloses the genetic material, and a smaller zone known as **nucleolus**. This subcompartment is not surrounded by a membrane and produces most of the ribosomal RNA. Adjacent to the nucleus we find the **Rough Endoplasmic Reticulum (ER)**, which processes and sorts out proteins (ER is a network of membrane-enclosed tubules and sacs). Generally rough ER has the largest membrane in

the cell structure; in contrast with smooth reticulum rough reticulum is studded with **ribosomes**. We could visualize see a ribosome like a protein synthesizer machine, it can synthesize a protein consisting of 100-200 amino acids in a minute or less, and a larger protein containing 30,000 amino acids in 2-3 hours. **Smooth ER** synthesizes fatty acids and phospholipids, and this organelle is present primarily in hepatocytes.

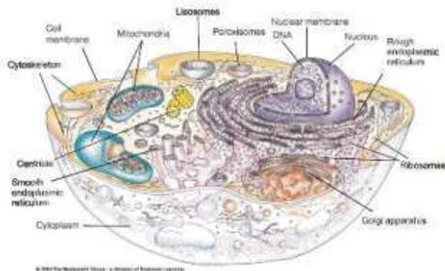


**Fig. 1.3** Image of Eukaryotic cell, the cell is surrounded by a plasma membrane, not indicated in the figure, and contains a nucleus, which is housed with a double membrane. The outer membrane is continuous and contains the rough endoplasmic reticulum, cytoskeleton, and cytoplasmic organelles like the Golgi apparatus which process and modify proteins. Mitochondria generate energy. Lysosomes digest cell materials to recycle them, peroxisomes process molecules using oxygen, and secretory vesicles carry cell materials to the surface in order to secrete them.

The proteins secreted from ER goes to the **Golgi apparatus**, and this flattened membrane processes and sorts the secreted proteins for transport to their destinations. This organelle modifies the vesicles that enclose the

proteins, the main functions of Golgi complex are: modification of substances synthesized by rough ER, cellular secretion, cytoplasmic membrane production and formation of primary lysosomes.

**Mitochondria**, other cellular organelles, are the main producers of energy derived from the breakdown of carbohydrates and fatty acids, which are transformed into ATP during an aerobic metabolism. Mitochondria are a large size organelles, and its dimensions are only exceeded by nucleus in animal cells. They have a double walled membrane, the outer membrane which defines the shape of the mitochondria, and this membrane is very similar to a gram positive membrane bacteria, and is freely permeable to all metabolites, but mainly to proteins. The inner membrane forms folds known as cristae and is extended along the interior of the organelle forming compartments that are the major working place in mitochondria. Mitochondria are the unique organelles within the cytoplasm of animal cell contain their own DNA.

Almost all human cells have these organelles, some exceptions are epidemic cells and erythrocytes, the first ones do not have the Golgi Apparatus, and the second ones do not contain nucleus. The evolution and cellular specialization results in a very complex variety of functions, shapes, sizes, compositions and mobilities.



## The cell membrane

The first interaction between exterior world and the cell occurs through the cellular membrane.

In particular the Cellular membrane separates interior of the cell from its environment. The membranes are based on simple bilayer structures, with phospholipids as fundamental building blocks. Phospholipids consist in two hydrophobic fatty acid chains joined to a hydrophilic phospholipid head groups (see Figure 1.4). The bilayer structure is maintained stable by hydrophobic and van der Waals interactions. This hydrophobic core is an impermeable barrier that prevents the diffusion of soluble solutes across the membrane.

In the bacterial membrane, the cell wall of Gram positive and negative is constituted of peptidoglycan of linear polysaccharide chains cross linked by short polypeptides. This characteristic is unique in bacteria and makes them vulnerable to some antibiotics.

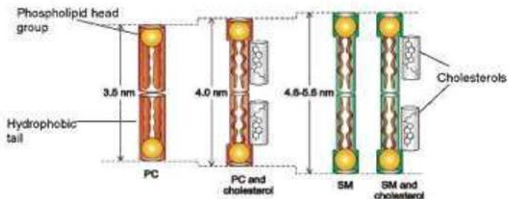


**Figure 1.4** Lipid composition of bilayer membranes. Pure sphingomyelin (SM) bilayer is thicker than one formed from a phosphoglyceride such as phosphatidylcholine (PC). Cholesterol has a lipid ordering effect of phosphoglyceride bilayers that increases the thickness but does not affect the thickness of more ordered SM bilayers. These dimensions are important for the phospholipid ordering through membranes and organelles. Adapted from [6]

The cell membrane is full of proteins, and represent 25 to 75% of the mass of all membranes. The membrane proteins feed the cell, expel harmful materials adhered on the surface or sense the environment. These proteins can interact with membranes in three different ways: *Integral membrane proteins*, they can cross the membrane, the domains outside the bilayer are hydrophilic, and the 3nm zone inside the bilayer is hydrophobic; *lipid anchored proteins*, they are anchored covalently to a one lipid molecule, the polypeptide chain do not enter in the bilayer; and *Peripheral membrane proteins* that do not interact with bilayers directly, they do so through lipid anchored membrane proteins, Figure 1.5 illustrates different membrane proteins inserted into lipid bilayer, and represents the configuration of proteins in lipid bilayers as a  $\beta$ -barrel.

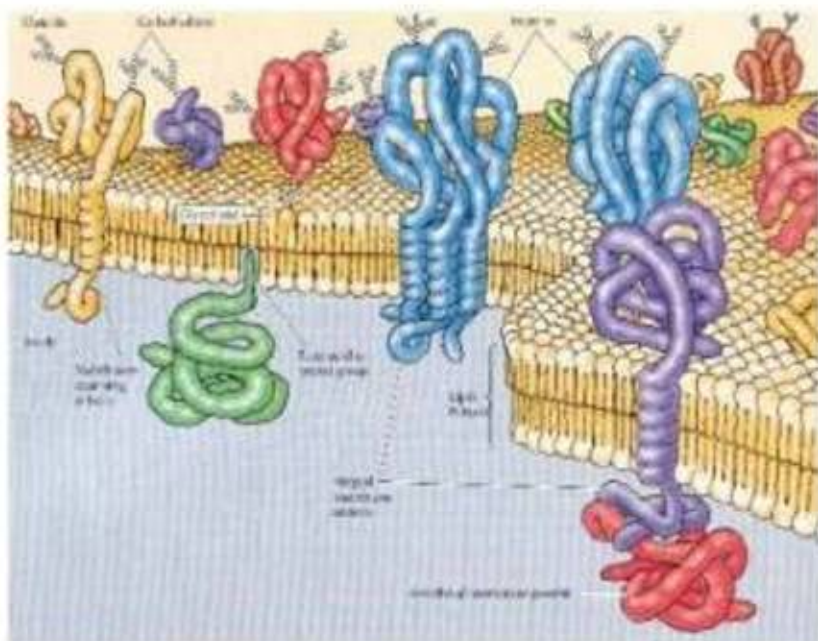


**Figure 1.5** Model of membrane structure. Taken from [Ref 3, pag 82]

Cells inside tissues could adhere one to other through four groups of integral membrane proteins called **immunoglobulin (Ig) superfamily**, **Cadherins**, **Integrins** and **Selectins** (Table 1.2). Cell adhesion mediated by selectins, integrins and cadherins requires  $\text{Ca}^{2+}$  or  $\text{Mg}^{2+}$ .

Integrins and Cadherins could function not only as cell adhesion molecules but also as signaling molecules that regulate cell proliferation and survival in response to cell-cell and cell-matrix contacts.

**Table 1.2 cell adhesion molecules (taken from [Ref 3, pag. 529])**

Family	Ligands recognized	Stable cell junctions
Selectins	Carbohydrates	No
Integrins	Extracellular matrix	Focal adhesions and hemidesmosomes
	Members of Ig superfamily	No
Ig superfamily	Integrins	No
	Homophilic interactions	No
Cadherins	Homophilic interactions	Adherens junctions and desmosomes

It is important to know which proteins are involved in adhesion and signaling processes because cancer cells have a poor adhesion to the matrix, causing metastasis and tumor proliferation, avokling dead cell signaling in and outside the cell (see below).

## Cellular cycle

Growth and reproduction are fundamental characteristics of all living organisms. Cells are also governed by this rule. The cell cycle regulates and coordinates the cell division, it is a process in which the cell passes through four stages. The main objective is generating daughter cells, the process of cellular division is known as **mitosis**. The cell cycle is divided in two parts mitosis and the interphase. For the interphase, the DNA and cells multiply their sizes. The four stages are differentiated by the amount of genetic material, which determines the nucleus size (Figure 1.6) In particular the **M** phase corresponds to mitosis, and in this phase the cell is divided in two

daughters, each daughter with identical genomic information; During the synthesis (S) phase the DNA is replicated. These two phases are separated by a gaps known as G1 in which the cell grows continuously but DNA does not grow, the cell is active metabolically, and in phase G2, the DNA has been duplicated and the cell keeps on growing; the cell synthesizes proteins for mitosis.

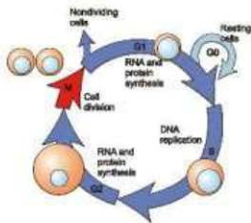
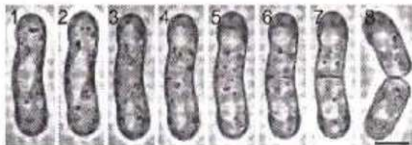


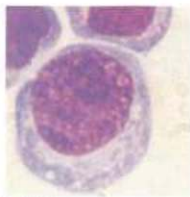
Figure 1.6. Stages of Eukaryotic cells during growth. In some conditions the cell alters duplication reaching a rest state known as G0. The quantity of genetic material is proportional to the nucleus size.

In multicellular organisms the cells allow the cell cycle to continue and keep resting for long periods, in few cases they only divide once, and rest all their life. This particular case occurs for nerves and ocular cells, and the post-mitotic state generally occurs after the G1 phase and is known as G0. The duration of the cell cycle depends on cell type and age. Generally under normal conditions the entire process takes from 10 to 20 hours, for example a human cell takes 24 hour to complete the cell cycle: mitosis takes 30 min, G1 takes ~9 hours, S ~10hours, and G2 ~ 4.5 hours. Yeast (see Figure 1.7) reproduces itself each 90 minutes, it means that in 24 hours a yeast cell replicates 16 times, and only one cell will produce ~65500 daughters.

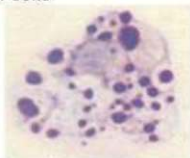
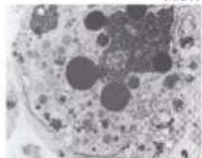


**Figure 1.7.** Successive phases in mitosis of yeast (*Saccharomyces pombe*), scale bar corresponds to 5  $\mu$ m. Taken from [Ref. 3, pag 596]

Cell replication has a limit because cells become old. On each replication there is a DNA lost. For example in eukaryote cells, chromosomes lost telomeres (a region of repetitive DNA at the end of chromosomes, which protects the end of the chromosome from destruction) every time they duplicate their DNA, and when telomeres length becomes short or chromosomal information is lost, the cell triggers a protection mechanism of self destruction named **Apoptosis**. In this way all organisms protect themselves from mutations, deformations and tumors. Another action that triggers apoptosis is virus infections, in this way cells prevent production of new virus particles and limit virus spread through the host organism. Apoptosis involves too many factors; chromosomal DNA is fragmented in small pieces, due to DNase action, and it is encapsulated by membrane fragments. Finally the whole cell is split in small apoptotic bodies enclosed by membranes. Figure 1.8 illustrates differences between two healthy human cells and their apoptotic counterpart. Apoptosis is known as a programmed cell death, and it is fundamental for all organ differentiation. There are other types of cell deaths such as **Necrosis**.



Normal cells



Apoptotic cells

**Figure 1.8** Optical and transmission electron micrographies of normal an apoptotic cells. In apoptotic cells it can be seen dark circles of compact chromatin when the nucleus starts to burst in apoptotic process. Images taken from [7]

Necrosis (accidental death) occurs when the tissue has been damaged, normally cells shrink or swell, releasing their content, commonly damaging neighbor cells and frequently cause inflammation.

## Cancer cells

Cancer constitutes a big and heterogeneous group of diseases, expressing an unbalanced relation proliferation/dead, causing genetic and epigenetic mechanisms. By altering the operation of some genes involved in cell proliferation, apoptosis, growth and DNA replication; the genes experience angiogenesis processes, invasion motility, adhesion and metastasis.

It is known that cancer cells seem to be immortal, this happens because each cell is able to replicate several times without affecting its life expectations. For example, some cancer cells can express the enzyme telomerase, replicate telomeres and avoid mechanisms that trigger apoptosis. There are six fundamental properties in cancer processes that are altered: self-sufficiency in growth signals, insensitivity to antigrowth signals, sustained angiogenesis, tissue invasion and metastasis, evasion of apoptosis and limitless replicative potential.

There is a large number of processes involved in carcinogenesis, many genes are activated producing new proteins and habituate processes that should be stopped, other genes are deactivated inhibiting some protein production or fail in regulatory cell cycle tasks.

Not all tumors are the same, there is not certainty that a drug eradicating a cancer type, is able to exterminate all cancers. For example cervical cancer differ among the same cervical tumors. In most cases cervical cancer starts with Human Papilloma Virus (HPV) infection, and there are more than 100



HPV known but only a few of those are of high risk and able to develop cancer. To mention some: HPV 16, 18, 33, 35, 39, 42, 52. So there exist differences among cervical cancers, and a cellular line culture known as CaSki is derived from an infection of the HPV 16. Another cervical cancer cell culture, HeLa (initials of Henrietta Lacks), is derived from the HPV 18.

In the same way cervix cancer is developed (e. g. via a virus) there are other causes that produce cancer such as genetic modifications, mutations, deletions and translocation. There are damages or mutations caused by external agents such as mutations by radiation, toxic issues, caused by bacteria (*helicobacterium pylori*, gastrointestinal cancer), fungi (*aspergillus flavus*, liver cancer) or viruses (*Hepatitis B, C*, liver cancer; HPV, cervix cancer).

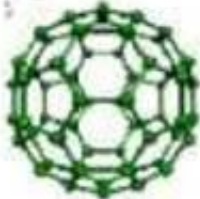


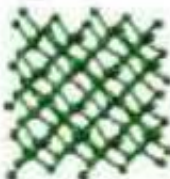
## Carbon Nanostructures. A brief review.

Carbon is one of the most abundant elements in the planet, all living organisms contain carbon. This element also presents a great affinity for a wide number of elements, making possible almost ten million of different compounds. All these variations provide the necessary constituents of living organisms, in the same way several of materials, such as polymers, contain mainly carbon atoms.

The carbon allotropes known before 1985 were graphite and diamond. However Sir H. Kroto *et al.* in 1985 discovered by accident a new allotrope of carbon: *fullerenes C<sub>60</sub>*, it has a soccer ball shape and is composed by 60 carbon atoms. Subsequently, S. Iijima in 1991, identified the chiral structure of carbon nanotubes, which can be considered as elongated fullerenes [8]. Following these achievements other nanostructures were proposed and/or synthesized, thus accelerating the nanocarbon field. The possibility of manipulating nanostructures opens up new avenues to synthesize novel materials with fascinating properties that are not present in bulk materials.

Because of the *C<sub>60</sub>* discovery it is now possible to make a list from zero dimensions to 3-dimensions isomers of carbon, as shown in table 1.3. Carbon is the only element having isomers.

Table 1.3 Carbon Isomers. Information taken from [9] and Images were taken from [10]

Dimensions	0-D	1-D	2-D	3-D
Isomer	$C_{60}$ fullerene	Nanotube, caynes	Graphite Fiber	Diamond amorphous
Hybridization	$sp^2$	$sp^2$ ( $sp$ )	$sp^2$	$sp^3$
Density (g/cm <sup>3</sup> )	1.72	1.2-2 2.68-3.13	2.26 ~ 2	3.515 2-3
Bond length (Å)	1.4 (C=C) 1.46 (C-C)	1.44 (C=C)	1.42 (C=C) 1.44 (C=C)	1.54 (C-C)
Electronic Properties	Semiconductor $E_g=1.9\text{eV}$	Metal or semiconductor	Semimetal	Insulating $E_g=5.47\text{eV}$
				

## Properties of Carbon Nanotubes.

A Carbon Nanotube (CNTs) can be viewed as rolled graphene sheet rolled or as an elongated fullerene. In general CNTs are classified in two different types: single-walled (SWNT), this kind of CNTs only contains an individual graphene sheet, and multi-walled (MWNTs), these tubes have two or more concentric graphene sheets. The properties of CNTs depends on the way the graphene sheet edges are arranged along the axis of the tube (chirality) (Fig. 1.9) In addition, geometrical defects in the hexagonal network are able to change chemical and physical properties of CNTs. A chiral carbon nanotube

is defined as the nanotube whose mirror image has not an identical structure, or both images cannot be superimposed. There are two cases for non-chiral carbon nanotubes: zig-zag and armchair. The names are due to the shape of the cross sections ring (see Figure 19).

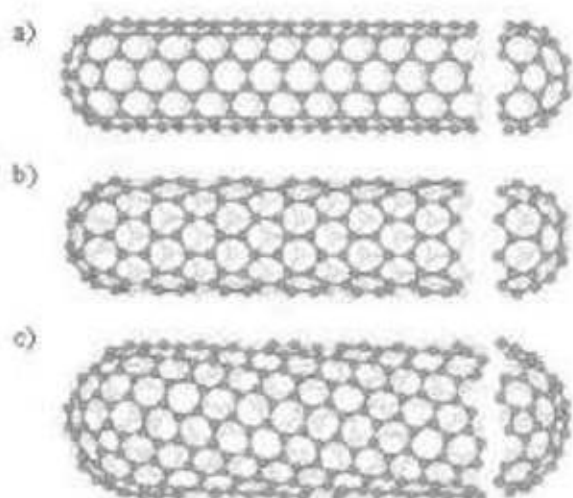


Fig 19: Classification of carbon nanotubes: a) armchair, b) zigzag and c) chiral. It can be seen the orientation of cross section carbon rings relative to the axis of the nanotube.

As is shown in Figure 1.10, the electronic properties change significantly depending how the graphene sheet is rolled. For an armchair CNT (Fig. 1.10 a)) there are states on Fermi level, making it a metallic material. However if the graphene sheets rolls up in a different way (Fig 1.10 b)), and the edges form a zigzag border, these tubes become semiconductors.

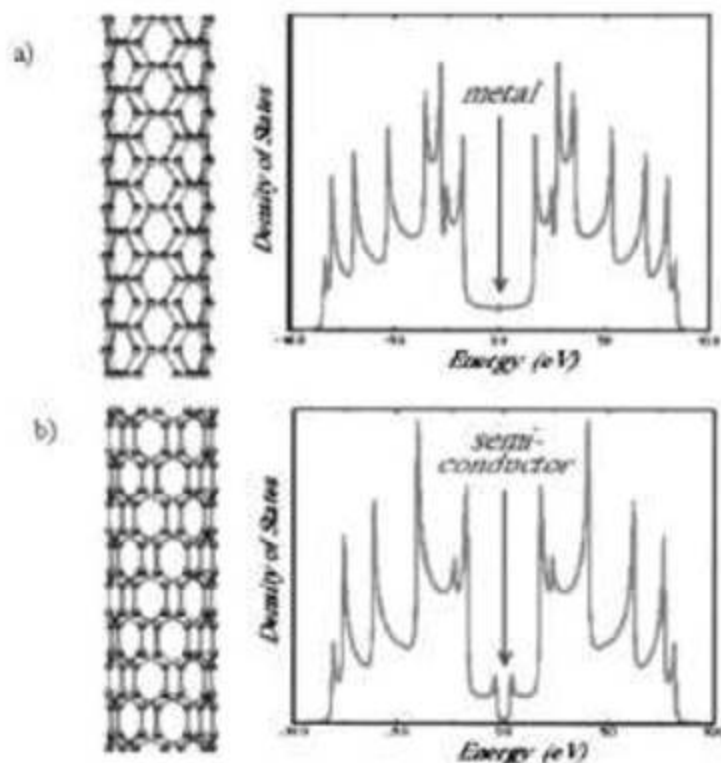
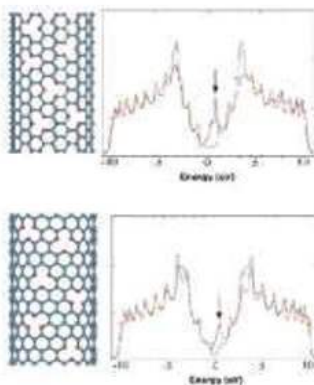


Figure 1.10 Density of states of (a) armchair carbon nanotube showing metallic properties, and (b) zigzag carbon nanotube, the narrow gap in Fermi level makes a semiconductor material Taken from [11]

The spectrum of possible applications and properties could increase if the CNTs are doped or functionalized. The introduction of different elements into the hexagonal array enables the possibility to control the physical and chemical properties. In Figure 1.11 a) one can observe an armchair CNT doped with nitrogen atoms, this modification breaks the hexagonal configuration, thus introducing novel properties. In Figure 1.11 b) one could note that the incorporation of nitrogen atoms in a zigzag CNT could result in a metallic tube due to the presence of electronic states on the Fermi level.



**Figure 11** Theoretical LDOS associated with a pyridine-like structure with N-doping carbon nanotubes displaying a armchair (10,10), and zigzag (17,0) configurations. In both cases, N atoms were placed randomly (N: red spheres; C: blue spheres, right hand edge). The LDOS of doped (black curve) and pure (red curve) carbon nanotubes are compared. It is clear that pyridine-like sites are responsible for the prominent donor-like features (plotted by arrows in the main picture) just above the Fermi energy. Taken from [12].

In addition to substitutional doping, functionalize CNTs surface by the acid treatment. These treatments enable dispersability of CNTs in polar solvents but the mechanical properties reduce.

## Synthesis, functionalization and bio-applications of Carbon Nanotubes.

The synthesis of CNTs are varied. Among them we could mention arc discharge [13][14], laser vaporization [15], electrolysis [16][17], pyrolysis of hydrocarbons [18]. These techniques have disadvantages and advantages related with impurities, crystallinity of the nanostructures, quantity, quality, costs and fabrication speed.

Pyrolytic decomposition of hydrocarbons, such as acetylene ( $C_2H_2$ ), benzene ( $C_6H_6$ ), carbon monoxide (CO), methane ( $CH_4$ ), known as chemical vapor deposition (CVD) technique, has become one of the most used methods for CNTs fabrication. CVD methods utilize the decomposition of hydrocarbon gases at elevated temperatures in the range 600–1200 °C. In this context, Endo *et al.* [19] reported the observation of nanotubes in the pyrolytic product of benzene ( $C_6H_6$ ) decomposition at about 1100 °C, Jose-Yacamán *et al.* [20] and Ivanov *et al.* [21] observed nanotubes in the catalytic decomposition of acetylene ( $C_2H_2$ ) at 1050–1350 °C, and Jaeger and Behring [22] found similar structures when using a mixture of natural gas, methane and benzene.

It is well known that CNTs of large diameter are inert, and this property prevents an easy dispersion of CNTs in any polar solvent (tubes are not reactive). In order to facilitate dispersability, diverse methods to functionalize CNTs surface are used.

The most common method to functionalize CNTs is by using strong oxidizing agents such as sulfuric ( $H_2SO_4$ ) and nitric ( $HNO_3$ ) acids. This treatment breaks the aromatic rings structure and introduces carboxylic groups on the open ends and help carrying further reactions enabling the dispersion. In this context, it has been reported amidation and esterification [23][24] in a relatively high temperature reaction.

Non-covalent functionalization can be achieved using  $\pi$ - $\pi$  stacking interactions between side walls of CNT and conjugated molecules such as those showed in Figure 1.12. Moreover, various lipids [25] and proteins [26] including enzymes [27], peptides [28] and nucleic acids [29], adsorb strongly to CNTs. These interactions provides more efficiency of solubilization in water than the use of surfactants and polymers

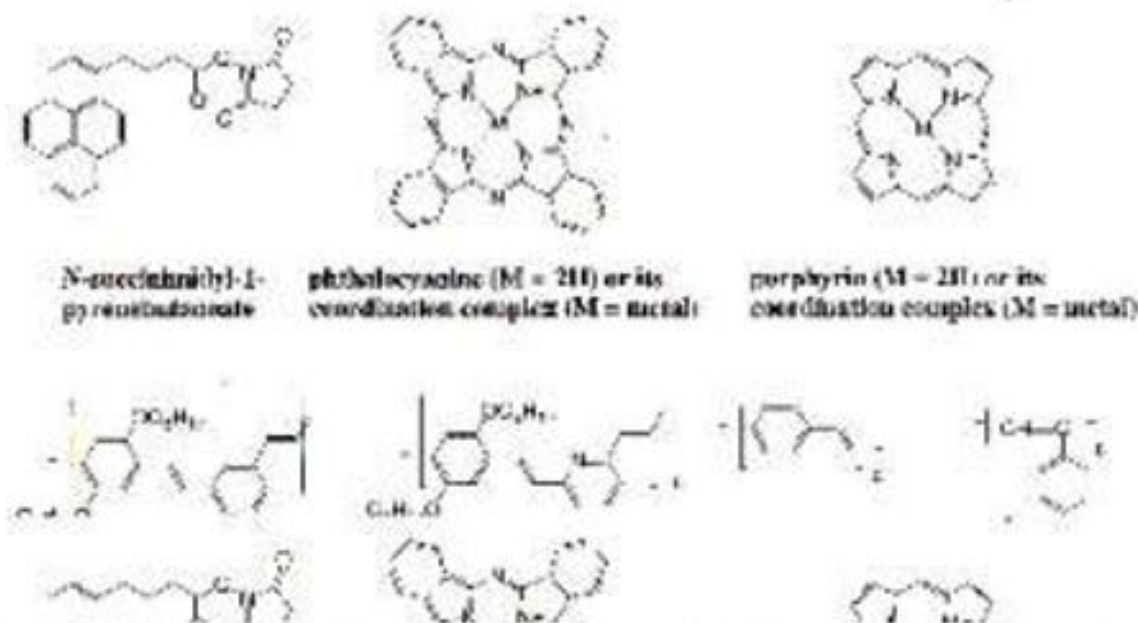


**Figure 1.12.** Typically molecules that can noncovalently modify CNTs via  $\pi$ - $\pi$  interaction. Taken from [30]



Functionalization of CNTs create polarity in charges, thus leading to an efficient separation from pristine tubules in polar solvents. This separation is desirable since it breaks the strong hydrophobic forces and van der Waals interactions among CNTs and make them more soluble, so that they could incorporate into biological systems.

The applications of Carbon Structures (CNS's) in biological organisms are extensive. For example, when sensing biomolecules, CNTs could serve as electronic devise in the biological recognition, CNTs could therefore be used as agent for identifying enzymes, antibodies, nucleic acids and aptamers. Some groups propose the use of CNTs as FETs (field emission transistor) or as nanoelectrode biosensors, and most groups involved in bioapplications, promote CNTs as drug delivery agent [31] or molecular transporters [32]. However, there are very few reports showing gene transfection or bacterial transformation [33][34].

The use of nanomaterials in medicine is becoming more important day by day. Unfortunately we do not know exactly all toxicological effects of nanomaterials. The enhanced rate area-volume (Figure 1.13) in nanostructures confers new properties. There fore, it is important to know how nanostructures interact with living cells and organisms.

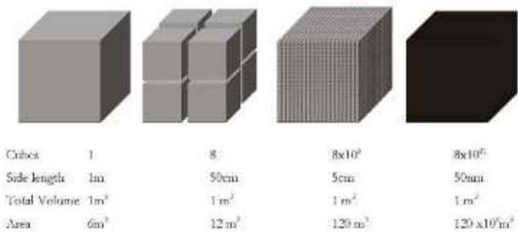


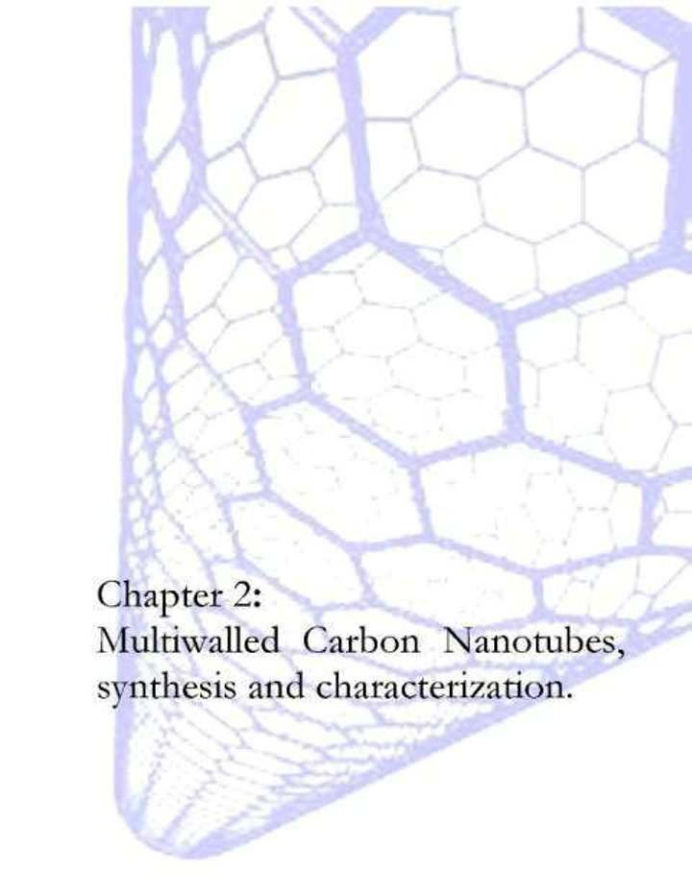
**Figure 1.13.** Importance of rate volume area in materials nanoengineered.

## References

- [1] Cross, P. C., Mercer, K. L.; *Cell and tissue Ultrastructure: A functional Perspective*. Ed. W. H. Freeman and Company, 1993.
- [2] Beck, A., Kausek, C. A., Lodish, H. F., Lodish, H., Darnell, J., Scott, M. P., Krieger, M., Matsudaira, P., Lawrence, S. *Molecular Cell Biology* W. H. Freeman and Company. (2003)
- [3] Cooper, M. G., Hausman, R. E. *The cell*, Sinauer Associates Inc.
- [4] Fredrickson, J. N., Zachara, J. M., Balkwill, D. L., Kennedy, D., Li, S. W., Kostandarithis, H. M., Daly, M. J., Romine, M. F., Bockman, P. J., Geomicrobiology of high-level nuclear waste-contaminated vadose sediments at the Hanford site, Washington state. *Appl Environ Microbiol* 2004, 70 (7): 4290-41.
- [5] Whitman, W., Coleman, D., Wiebe, W. Prokaryotes: the unseen majority. *Proc Natl Acad Sci USA* 95 (12): 6578-83, 1998.
- [6] Sprong, H., Sluijs, P., Meer, G.; How proteins move lipids and lipids move proteins. *Nature Reviews Molecular Cell Biology* 2, 504-513.
- [7] Arends, M. J., Wyllie, A. H. Apoptosis: Mechanisms and roles in pathology. *Int Rev Exp Pathol* 32:223.
- [8] Enko, M., Krotov, W. H., Formation of carbon nanofibers. *J. Phys Chem*, 1992, 96, 6941-6944.
- [9] Saito, R.; Dresselhaus, G. Dresselhaus, M., *Physical Properties of Carbon Nanotubes*. Imperial College Press: London, United Kingdom, 1998.
- [10] Lepko, N. N., Attachment of transition metal nanoparticles on nitrogen doped carbon nanotubes (MWNTEs/CNx) and their further reactions. *ITC/T Advanced materials thesis*.
- [11] Terrones, M., Carbon nanotubes: synthesis and properties, electronic devices and other emerging applications. *International Materials Reviews*. 2004 Vol 49 No 6, 325-377.
- [12] Terrones, M., Ajayan, P.M., Banhart, F., Blase, X., Carroll, D. J., Charlier, J.C., Czerw, R., Foley, D., Grobert, N., Kamalekan, R., Kohler Redlich, P., Röhle, M., Seeger, T., Terrones, H. N-doping and coalescence of carbon nanotubes: synthesis and electronic properties. *Appl Phys A*. 2002 74, 355-361.
- [13] Iijima, S. Helical microtubules of graphitic carbon. *Nature*, 1991, 354, 56-58.
- [14] Kratschmer, W., Lamb, L. D., Fostiropoulos, K., Huffman, D. R. Solid C60: a new form of carbon. *Nature*, 1990, 347, 354-358.

- [15] Guo, T., Nikolaev, P., Rinzler, A. G., Tomazek, D., Colbert, D. T., Smalley, R. E. Self-Assembly of Tubular Fullerenes *J. Phys. Chem.*, 1995, 99, 10694-10697.
- [16] Iijima, W. K., Hare, J. P., Terrones, M., Kroto, H. W., Walton, D. R. M., Harris, P. J. Condensed phase nanotubes. *Nature*, 1995, 377, 687-687.
- [17] Hsu, W. K., Hare, J. P., Terrones, M., Kroto, H. W., Walton, D. R. M., Harris, P. J. Electrolytic formation of carbon nanostructures. *Chem. Phys. Lett.*, 1996, 262, 161-166.
- [18] Dresselhaus, M. S., Dresselhaus, G., Sughara, K., Spain, I. I., Goldberg, H. A., *Graphite fibers and filaments*. Vol. 3, Chap. 2, 12; 1988, Berlin/New York/London, Springer.
- [19] Endo, M., Takeuchi, K., Igarashi, S., Kobori, K., Shirahata, M., Kroto, H. W., The production and structure of pyrolytic carbon nanotubes (PCNTs). *Phys. Chem. Solids* 34 (1993) 1841-1848.
- [20] Yacaman, M. J., Miki-Yoshida, M., Rendon, L., Santesteban, J. G. Catalytic growth of carbon microtubules with fullerenic structure. *Appl. Phys. Lett.* 62 (1993) 657-659.
- [21] Ivanov, V., Nagy, J. B., Lambin, Lucas, A., Zhang, X. D., Zhang, X. F., Emmerits, Van Tendeloo, G., Amelincx, S., Van Landuyt. The study of carbon nanotubules produced by catalytic method. *J., Chem. Phys. Lett.* 225 (1994) 329-335.
- [22] Jaeger, H., Behring. Novel microstructure transformation of benzene-derived carbon filaments under laser irradiation. *Compos. Sci. Technol.* 51 (1994) 231-234.
- [23] Noyce, S., Hamon, M. A., Hu, H., Zhao, B., Bhowmik, P., Sci, R., Itkis, M. E., Haddon, R. C. Chemistry of single walled carbon nanotubes. *Acc. Chem. Res.* 2002, 35, 1108-1113.
- [24] Sun, Y. P., Fu, K., Lin, Y., Huang, W. Functionalized Carbon nanotubes: properties and applications. *Acc. Chem. Res.* 2002, 35, 1096-1104.
- [25] Richard, C., Balavoine, F., Shultz, P., Elbreen, T. W., Miskowski, C. Supramolecular self assembly of lipid derivatives on carbon nanotubes. *Science*, 2003, 300, 775-778.
- [26] Balavoine, F., Schiltz, P., Richard, C., Mallohi, V., Elbreen, T. W., Miskowski, C. Helical Crystallization of proteins on carbon nanotubes: a first step towards the development of new biosensors. *Agnew. Chem. Int. Ed.* 1999, 38, 1912-1915.
- [27] Besteman, K., Lee, J.-O., Wiertz, F. G., Heering, H. A., Dekker, G. Enzyme-coated carbon nanotubes as single molecule biosensors. *New letters*, 2003, 3, 727-730.
- [28] Zorbas, V., Ortiz-Accredo, A., Dalton, A. B., Yoshida, M. M., Dieckmann, G. R., Draper, R. K., Baughman, R. H., Jose Yacaman, M., Muechman, I. H. Preparation and

- characterization of individual peptides grafted single walled carbon nanotubes. *J. Am. Chem. Soc.* 2004, 126, 7222-7227.
- [29] Zheng, M., Jagota, A., Strano, M. S., Santos, A. P., Barone, P., Grace Choi, S., Diner, B. A., Dresselhaus, M. S., Meloni, R. S., Bittara Onoa, G., Samsonidze, G. G., Semke, H. D., Urey, M., Walk, D. J. Structure based Carbon nanotube sorting by sequence-dependent DNA assembly. *Science* 2003, 302, 1545-1548.
- [30] Alberto, B., Wei, W., Giogias, P., Cedric, K., Lars, I., Charalambos, D. P., Krstas, K., Marzio, Pato. 2007, cap 3, pag 87; *Nanomaterials for medical diagnosis and therapy*.
- [31] Pantarotto, D., Singh, R., McCarthy, D., Ehrhardt, M., Briand, J-P., Pato, M., Kostarelos, K., Bianco, A. Functionalized Carbon Nanotubes for Plasmid DNA Gene Delivery. *Angew. Chem. Int. Ed.* 2004, 43, 5242-5246.
- [32] Naeini, W., Theodore, C. J., Paul A. W., Horigie, D. Nanosize Molecular Transporters: Internalization of Carbon Nanotube-Protein Conjugates into Mammalian Cells. *J. Am. Chem. Soc.* 2004, 126, 6850-6851.
- [33] Rojas-Chapman, J., Troxczynska, I., Fekirska, I., Morasock, C., Gierzig, M. Multi-walled carbon nanotubes for plasmid delivery into *Escherichia coli* Cells. *Lab. Chip.* 2005, 5, 536-539.
- [34] Del Rio, E., Galvan, F., de Leon Rodriguez, A., Barba de la Ross, A. P., Texcones, M., to be submitted.



Chapter 2:  
Multiwalled Carbon Nanotubes,  
synthesis and characterization.

In chapter 1 we discussed the complexity and properties of CNTs upon their morphology. These characteristics could vary drastically when a different element or elements are embedded in the hexagonal network of the nanotubes. It is worth mentioning that during synthesis using Chemical Vapor Deposition (CVD) approach, structures defects are created on the surface of the tube and these could also affect the nanotube properties and performance.

## Nanotube Synthesis

In this thesis we synthesized three different types of CNTs: Multiwalled CNTs (MWNTs), Multiwalled CNTs doped with Nitrogen (CNx-MWNTs) and Multiwall CNTs functionalized with carbonyl radicals (COx-MWNTs).

MWNTs were synthesized by the CVD method. In particular this process consists in generating an aerosol from a solution containing an organometallic precursor and a hydrocarbon (solvent). The solution composition for synthesizing MWNTs is 2.5% wt. of ferrocene (Aldrich ®, cat: F408-500G) and 97.5% wt. of toluene (Fermont ®, cat 06605). For the synthesis of CNx-MWNTs the solution composition corresponds to 2.5% wt. ferrocene (Aldrich ®, cat: F408-500G) and 97.5%wt benzylamine (benzylamine reagent plus 99%, Sigma-Aldrich ®, cat 185701-500G). Finally for producing COx-MWNTs the solution composition used was 2.5% wt. ferrocene (98% Aldrich ®, cat: F408-500G), 96.5% wt Toluene (Fermont ®, cat 06605) and 1%wt ethanol (CTR scientific ®) [1]. The process is described by Pinault et al elsewhere [2]. The synthesis setup is described in Figure 2.1 and this technique was used for producing all nanotubes samples described in this thesis. The experimental conditions for producing the nanotube samples were, the first furnace temperature was 820°C and the second furnace 800°C, While heating, the argon flow corresponded to 0.5 L min<sup>-1</sup>, and during the nanotube synthesis, the flow was increased until reaching 2.5 L min<sup>-1</sup>, the time of synthesis for MWNTs and CNx-MWNTs samples was set for 30 min, and 15 minutes for COx-MWNTs.

Once the nanotube synthesis takes place, the furnaces were cooled down to room temperature slowly, the sprayer is turned off and the flow is down to 0.5 L min<sup>-1</sup>. Subsequently we scaped the quartz tube walls in order to obtain the black carbonaceous flakes containing the nanotube material.



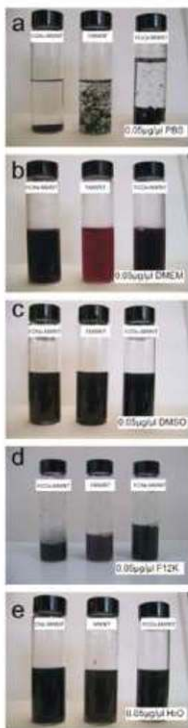
# Functionalization, cleaning and dispersion of Carbon Nanotubes

Pristine CNTs contain impurities, such as amorphous carbon, metallic nanoparticles and un-reacted solvents. These undesired materials lead to different results in our studies with biological samples.

Therefore, it is important to eliminate impurities and obtain nanotube samples presenting clean surfaces that could be used with biomolecules.

In addition, CNTs must be dispersed uniformly in liquids for studying interaction with biological systems; this means that it is necessary to have hydrophilic CNT surfaces in order to obtain a good dispersion in a cell culture medium, buffer or water.

In order to achieve nanotube functionalization and hydrophilicity we employ an oxidation treatment using sulfuric and nitric acids, with a [3:1] ratio respectively. As explained by Jie Liu et al. [3], the procedure consists of sonicating the acid dispersions with nanotubes and for 2 hours. In particular, 50 mg of CNTs are weighted and mixed with this acid solution. Note that this is a strong reaction and toxic vapors could be released. Therefore and in order to avoid health hazards, the acid treatment must be carried out inside an extraction hood.



To remove the acid from this suspension we dissolved the sample in 500 mL double deionized water, and proceeded to filter the material, using a 200nm pore membrane. Once filtered, 500ml of NaOH 1M was added in order to neutralize all acid residues, Subsequently the sample was washed twice with double deionized water, and the material let to dry at room temperature.

Tests in polar solvents were carried out in diverse cell culture medium, buffer and water. Figure 2.1 shows the dispersibility of functionalized CNTs in diverse solvents, and all samples have a concentration of  $50 \mu\text{g mL}^{-1}$ . It is easy to note that  $f\text{CNx-MWNT}$

**Figure 2.1** Dispersibility tests in different solvents for  $f\text{CNx-MWNT}$ ,  $f\text{CCx-MWNT}$  and  $f\text{MWNT}$ . Picture **a** shows bad dispersability in Phosphate buffer solution (PBS), it is evident the agglomeration of CNTs. Figures **b**, **c**, **d** and **e** shows a very good dispersion in Dulbecco's Modified Eagle's Medium (DMEM), Dimethyl Sulfoxide (DMSO), F12K medium and double distilled water respectively. All samples have a concentration of  $50 \mu\text{g mL}^{-1}$  and were ultrasonicated from 15 to 45 minutes depending on the time that CNTs disperse homogeneously in solvents.

presents more affinity for solvents than  $f$ -MWNT and  $f$ -CO<sub>x</sub>-MWNT.

The solvents used were selected having in mind their use in diverse cellular cultures, thus suggesting some applications, such as bacterial transformations in which plasmid DNA are treated with CNTs dispersed in water or PBS.

## Nanotubes Characterization

Pristine CNTs and acid treated CNTs were characterized by scanning electron microscopy (SEM) Energy Dispersion X-Ray analysis (EDX), Raman spectroscopy.

### Scanning Electron Microscopy and Energy Dispersive X-ray Analysis

Tables 2.1, 2.2 and 2.3 shows EDX results of pristine MWNTs, CN<sub>x</sub>-MWNT, and CO<sub>x</sub>-MWNT, respectively. The tables indicate data of different zones within each sample. Although, Fe is usually encapsulated inside carbon nanotubes, some cells could be sensitive to these encapsulated nanoparticles [4]. To know the Fe percentage we made a detailed EDX analysis.

**Table 2.1.** Elemental analysis of EDX for pristine MWNT.

Element	MWNT zone 1		MWNT zone 2		Average	
	Wt %	At %	Wt %	At %	Wt %	At %
C	94.86	97.81	95.88	97.69	95.27	97.75
O	1.81	1.41	2.57	1.97	2.19	1.80
Fe	3.53	0.78	1.55	0.34	2.54	0.56
Total	100	100	100	100	100	100

**Table 2.2** Elemental analysis of EDX for pristine CNx MWNT.

Element	CNx zone 1		CNx zone 2		CNx zone 3		Average	
	Wt %	At %	Wt %	At %	Wt %	At %	Wt %	At %
C	87.06	94.54	92.38	95.54	92.38	94.71	90.60667	94.93
N	2	1.86	2.34	2.07	3.03	2.66	2.456667	2.196667
O	1.79	1.40	2.18	1.7	2.94	2.27	2.303333	1.81
Fe	9.14	2.14	3.1	0.69	1.65	0.36	4.63	1.063333
Total	99.99	100	100	100	100	100	99.99667	100

**Table 2.3** Elemental analysis of EDX for pristine COx-MWNT.

Element	COx-MWNT zone 1		COx-MWNT zone 2		Average	
	Wt %	At %	Wt %	At %	Wt %	At %
C	94.7	97.31	95.25	97.61	94.975	97.46
O	2.74	2.12	2.43	1.87	2.585	1.995
Fe	2.56	0.67	2.32	0.51	2.44	0.54
Total	100	100	100	100	100	100

Tables 2.4, 2.5 and 2.6 illustrate EDX spectra information of the elements present within all samples (pristine and functionalized).

**Table 2.4.** Elemental analysis of EDX for *f*-MWNT after 2 hours of acid treatment

Element	<i>f</i> -MWNT zone 1		<i>f</i> -MWNT zone 2		Average	
	Wt %	At %	Wt %	At %	Wt %	At %
C	90.46	94.12	89.7	93.16	90.08	93.64
N	0.67	0.77	1.23	1.09	1.05	0.93
O	4.95	3.88	6.79	4.51	5.375	4.195
Na	1.15	0.62	1.48	0.8	1.315	0.71
S	0.21	0.06	0.2	0.08	0.205	0.08
Fe	2.36	0.53	1.61	0.36	1.985	0.445
Total	100	100	100	100	100	100

**Table 2.5** Elemental analysis of EDX for *f*/CNx MWNT after 2 hours of acid treatment

Element	<i>f</i> CN <sub>x</sub> -MWNT zone 1		<i>f</i> CN <sub>x</sub> -MWNT zone 2		<i>f</i> CN <sub>x</sub> -MWNT zone 3		<i>f</i> CN <sub>x</sub> -MWNT zone 4		<i>f</i> CN <sub>x</sub> -MWNT zone 5		Average	
	Wt %	At %	Wt %	At %	Wt %	At %	Wt %	At %	Wt %	At %	Wt %	At %
C	83.41	87.91	83.46	88.17	87.11	91.22	87.12	90.71	87.67	91.53	85.754	89.908
N	3.47	3.14	2.92	2.64	1.39	1.24	1.75	1.57	1.82	1.63	2.27	2.044
O	9.44	7.47	9.03	7.04	8.05	6.34	8.96	7.01	7.32	6.74	8.682	6.84
Na	1.62	0.89	1.05	0.91	0.59	0.32	0.39	0.21	0.59	0.32	0.968	0.53
S	0.75	0.3	0.66	0.26	1.4	0.55	0.87	0.26	1.17	0.46	0.93	0.366
Fe	1.31	0.3	1.88	0.38	1.45	0.33	1.11	0.25	1.43	0.32	1.396	0.316
Total	100	100	100	100	100	100	100	100	100	100	100	100

**Table 2.6** Elemental analysis of EDX for *f*-MWNT after 2 hours of acid treatment

Element	<i>f</i> -CO <sub>x</sub> -MWNT zone 1		<i>f</i> -CO <sub>x</sub> -MWNT zone 2		Average	
	Wt %	At %	Wt %	At %	Wt %	At %
C	91.27	95.2	90.9	94.92	91.085	95.06
N	1.16	1.03	1.08	0.97	1.12	1
O	2.96	2.32	3.38	2.65	3.17	2.485
Na	1.03	0.56	1.04	0.57	1.035	0.565
S	0.49	0.19	0.62	0.2	0.505	0.195
Fe	3.09	0.69	3.07	0.89	3.08	0.69
Total	100	100	100	100	100	100

Many authors indicate that the oxidation treatment with sulfuric and nitric acids functionalize CNTs walls with carbonyl, carboxyl, hydroxyl and sulfur groups. If we compare the tables, it can be seen the addition of new elements and for CN<sub>x</sub>-MWNTs and pure carbon MWNTs, the Fe rates decrease.

Table 2.7 indicates the summary of EDX elemental characterization for pristine and oxidized CNTs, in this table it is easier to analyze the elemental variations.

**Table 2.7** Overview of results from EDX characterization

Treatment	EDX					
	Be %	C %	O %	S %	N %	Ka %
Pristine MWNT	2.51	95.27	2.19	-	-	-
SiO <sub>2</sub> /CNT	1.985	90.68	5.375	0.268	1.65	1.315
Pristine-CNOx/MWNT	4.63	90.60	2.30	-	2.45	-
f-CNOx/MWNT	1.506	85.754	8.682	0.93	2.27	0.968
Pristine-COx/MWNT	2.44	91.975	2.585	-	-	-
fCOx-MWNT	3.08	91.685	3.17	0.565	1.12	1.035

In Figures 2.2 we can evaluate dispersability of CNTs in water (hydrophilicity). The CNTs samples dispersed in solvents and few droplets were deposited on a silicon substrates and let overnight for SEM studies.

It is noteworthy that functionalized CNTs in PBS do not show a good dispersability, the tubes tend to agglomerate and precipitate after one hour.

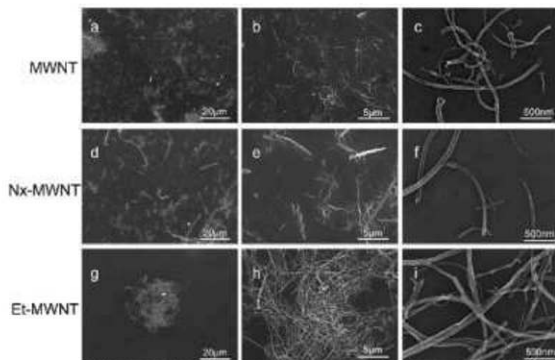


**Figure 2.2.** CNTs dispersed in double distilled water. In Figures a, b and c fMWNT reveal a good dispersion. Figures d, e and f illustrate again a good dispersion for fCNx-MWNTs, and finally, Figures g, h and i illustrate a bad dispersability of fCOx-MWNTs.

In order to determinate the CNTs dispersability in cell culture medium it is necessary to use Scanning Transmission Electron Microscopy (STEM). The thickness of the dry medium hides CNTs into it, so electronic transmission microscopy aids to observe how CNTs immerse in bio-cells. The Figure 2.3 shows SEM and STEM images of CNTs dispersed in DMEM, it can be seen CNTs perfectly embedded and dispersed in medium.

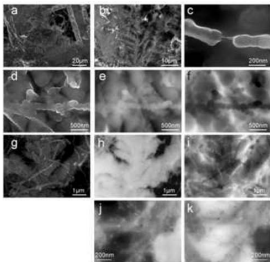
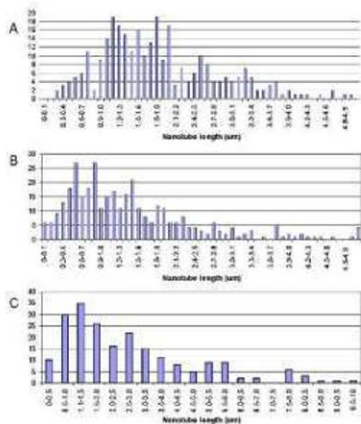


**Figure 2.3** SEM and STEM images of /CNs-MWNTs in DMEM. a, b, and c are SEM images, it can be seen the thickness of dry DMEM, a and b, and a almost completely covered CNT in c, this tell us about the functionalization through the CNT surface and affinity for medium. Images d and f are SEM images and e, f and h, i are their STEM images respectively in dark and light phase, were shows CNTs inside of the medium scab. Images j and k are the same zone in different phases and an iron particle can be seen with high contrast inside of a CNT.



According to Jie Liu et al, acid treatments cuts CNTs, this process is important due to the cell size; short nanotubes will interact better than long nanotubes. Graphs 2.1, 2.2 and 2.3 reveal the statistical length of CNTs length after the oxidation treatment



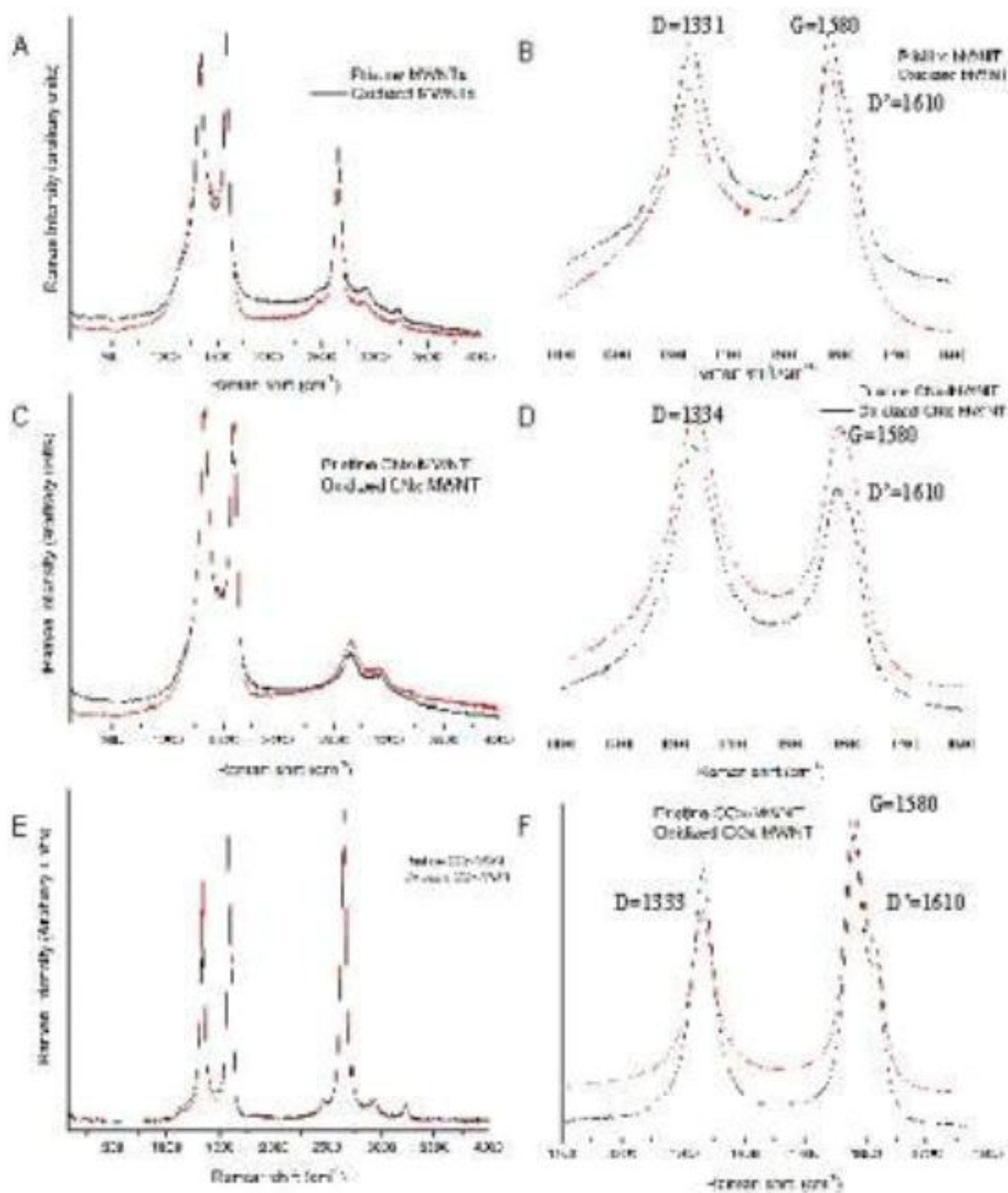
**Graphic 2.1** Length distribution plots of cut nanotubes after storing in a 3:1 mixture of sulfuric and nitric acid for 2 hours. The average length after acid treatment of MWNTs (A) is approximately 1.5 µm, for CNx-MWNTs (B) the average length is 0.8 µm and 1.4 for COx MWNTs (C).

## Raman spectroscopy

In general, the Raman spectra of raw and treated CNT samples are composed of two characteristic peaks: the G-band near  $1580\text{ cm}^{-1}$  and the D-band located at  $1350\text{ cm}^{-1}$ . The G-band is related to the graphite  $E_{2g}$  symmetry of the interlayer mode, which reflects the structural intensity of the  $sp^2$ -hybridized carbon atoms of the nanotubes. The D-band is a result of the disordered carbon atoms when the hexagonal symmetry of graphite is broken. The extent of the defects in carbon nanotubes can be evaluated when using the ratio of the D and G band intensities ( $I_D/I_G$ ) [5].

In plots depicted in Figures 2.2 A, C, and E seem to be similar in both curves, pristine and treated MWNs. However by making a zoom in D ( $1350\text{cm}^{-1}$ ), G ( $1580\text{cm}^{-1}$ ) and D' ( $1610\text{cm}^{-1}$ ) bands (see Figures B, D and F), small changes in the D' band for oxidized curves occur, (see Rosca et al [6]), Figure 2.4, the crystalline graphitic structure is gradually altered as the relative areas of the G and D) band change visibly.

These results are in agreement with the results reported by Musso et al, indicating that a few changes in morphology are visible after  $\text{H}_2\text{SO}_4/\text{HNO}_3$  treatment, except for D' band, in which the change is notably.



**Graphic 2.2** Experimental Raman spectrum taken with an Ar<sup>+</sup> ion laser at 514.5nm wavelength excitation from 3 samples: MWNT (A, B), CN<sub>x</sub>-MWNTs (C, D) and CO<sub>x</sub>-MWNT (E, F). A zoom are made for a range of 1100 to 1800 cm<sup>-1</sup> for these CNTs types, showing magnifications of D, G and D' bands.

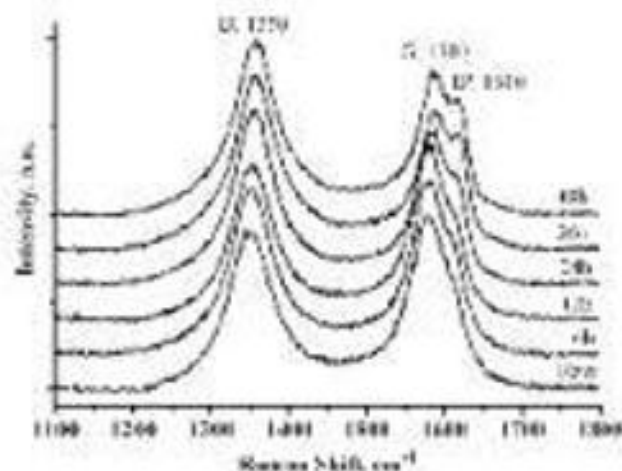


**Figure 2.4** Series of Raman spectra of the MWCNT oxidation. MWCNT = 10 mg/ml; HNO<sub>3</sub> = 60%. Taken from [7]

Usually the  $I_D/I_G$  ratio is taken as a measure of defect concentration. It has been argued that the G mode in the Raman spectra of carbon nanotubes originates from a defect induced double resonance scattering process [8]. In order to obtain reliable information about the defect density it is necessary to include the intensity of the second order overtone mode  $D'$ , which is due to two phonon processes and hence to first approximation independent of defect concentration [9]. In order to clarify elucidate this controversy, in Table 2.8 are show the relative intensities  $I_D/I_G$ ,  $I_G/I_D$ , and  $I_D/I_G'$  of the Raman peaks as a function of treatment condition using a 514.5 nm excitation wavelength.

**Table 2.8** Relative intensities  $I_G/I_D$ ,  $I_G/I_D'$ ,  $I_D/I_G'$  of the Raman peaks for pristine and oxidized CNTs using a 514.5 excitation wavelength

Treatment	Raman		
	$I_G/I_D$	$I_G/I_D'$	$I_D/I_G'$
Pristine MWNT	0.8887		
βMWNT	0.6581		
Pristine CNx-MWNT	0.8633		
βCNx-MWNT	0.9455		
Pristine COx-MWNT	0.92186	1.5168	1.7066
βCOx-MWNT	0.9636	1.1829	1.69678

## References

- [1] Botello-Mendez, A., Campos-Delgado, J., Morelos-Gomez, A., Rodriguez A. G., Navarro, H., Vidal, M. A., Terrones, H., Terrones, M., Controlling the dimensions, reactivity and crystallinity of multiwalled carbon nanotubes using low ethanol concentrations, *Chem. Phys. Lett.* 453, (2008) 55–61.
- [2] Pinault, M., Mayne-L, M. Reynaud, Pichot, V., Lannois, P., Ballutaud D Growth of multiwalled carbon nanotubes during the initial stages of aerosol-assisted CCVD; *Carbon* 43, (2005) 2968–2976.
- [3] Liu, J., Andrew G. Rinzler, Dai, H., Jason H. Hafner, R. Bradley, K., Peter J. Boul, Lu, A., Iverson, T., Shelimov, K., Huffman, B. C., Rodriguez-Macias, F., Shon, Y-S., Randall Lee, T., Colbert, D. Y., Smalley, R. E. Fullerene Pipes, *Science*, 280, 1253-1256
- [4] Uo, M., Tamura, K., Sato, Y., Yokoyama, A., Watari, F., Totsuka, Y., Tohji, K., The toxicity of Metal-encapsulating carbon nanocapsules. *Small*, (2005) 1, No 8-9, 816-819.
- [5] Musso, S., Porro, S., Vianic, M. Vanzetti, L., Ploger, R., Giorelli, M., Possetti B., Trotta, F., Pederzoli, C., Tagliaferro, A., Modification of MWNTs obtained by thermal-CVD, *Diamond & Related Materials* 16 (2007) 1183–1187
- [6] Bacsa W.S., Ugarte, D., Chatelain, A., de Heer, W. A. High-resolution electron microscopy and inelastic light scattering of purified multishelled carbon nanotubes. *Phys. Rev.* (1994) B50: 15473–15476.
- [7] Rosca, I. D., Watari, F., Uo M., Akasaka, T., Oxidation of multiwalled carbon nanotubes by nitric acid, *Carbon* 43, (2005) 3124–3131.
- [8] Maultzsch, J., Reich, S., Thomsen, C., *Appl. Phys. Lett.* 81, 2647 2002.

- [9] Murphy, H., Papakonstantinou, P., Okpalugo, T. I. T. Raman study of multiwalled carbon nanotubes functionalized with oxygen groups, *J. Vac. Sci. Technol. B*, 2006, 24, 2, 715-720
- [10] Felten, A., Hody, H., Bittencourt, C., Pireaux, J. J., Hernández Cruz, D., Hitchcock, A. P., Scanning transmission x-ray microscopy of isolated multiwall carbon Nanotubes, *Appl Phys Lett* (2006) 89, 093123.
- [11] Felten, A., Bittencourt, C., Pireaux, J.-J., Reichelt, M., Mayer, J., Hernandez-Cruz, D., Hitchcock, A. P., Individual Multiwall Carbon Nanotubes Spectroscopy by Scanning Transmission X-ray Microscopy, *Nano Lett* (2007) Vol. 7, No. 8, 2937-2941.

A microscopic image showing a cell on the left side, stained in a light blue color. A prominent, elongated, and slightly curved structure extends from the cell towards the center of the frame. The background is mostly white with some faint blue specks.

Chapter 3:  
Interaction between Human  
Cells and Multiwalled Carbon  
Nanotubes

Different cell types have been treated with different types of CNTs in order to explain or study the interaction between both systems. Generally, in order to study interactions *in vitro* of cells, scientists use modified or immortal cellular lines. For example: a) human epidermal keratinocytes (HaCaT); b) human dermal fibroblasts (HDF) that are derived from the dermis of normal human neonatal foreskin or adult skin; this cell line is cryopreserved at the end of primary culture and could be cultured and propagated in at least 16 population doublings; c) Cervical cancer cells such as HeLa; (cell culture taken from a woman named Henrietta Lacks who died due to her cancer in 1951), and d) CaSki cells which were established as a cell line from an epidermis carcinoma of the human cervix in 1977 by Parillo et al. [1]; e) Human embryo kidney (HEK) cells, a culture modified by an adenovirus type 5 in 1970 by Van der Eb [2]. All these cell lines are widely used in cell biology research.



Several papers have reported the interactions between cells and Carbon Nanostructures [3]. In this context Jia et al. (2005) observed a reduction of 20% in cell viability of alveolar macrophages due to possible impurities present in SWNTs [4]. The group of Ramesh, [5] in 2005 reported an increase of HaCaT cell death possibly due to an oxidative stress of pristine SWNTs or induced by solvent contamination contained in the tubes. Bottini et al, [6] compare the toxicity of pristine and oxidized MWNTs on human T cells and found that the latter are more toxic, they use high concentrations of CNTs. Shvedova et al. [7] reported a morphological changes in the same cell culture when the cells were treated with pristine HiPCO (high-pressure carbon monoxide)-SWNTs. In 2006, Sayes et al. [8] observed toxicity *in vitro* of functionalized SWNTs on HDF cell cultures. These authors found a 50% (or below) of cell deaths. In the same year Dumortier et al, [9] reported the impact of functionalized CNTs on cells of the immune system, and found no influence on cell viability. Sato's group [10] also reported the influence of an inflammatory response in subcutaneous tissue in rats caused by MWNTs of 825 nm in length; however Kiura et al. [11] reported an effect of immune response in the same cell line with SWNTs synthesized by arc discharge and CVD methods. Kobayashi et al, [12] found that refined SWNTs are more toxic than other carbon nanomaterials. Interestingly, Pantarotto et al. [13] reported a rapid uptake of functionalized SWNTs by fibroblasts, and observed a non remarkable cell death. The same group also used the same CNTs and functionalized MWNTs for plasmid delivery onto HeLa cells, without cellular death [14]. Some studies have been carried out with HEK and; the group of Leong [15] used MWNT-PEI (poly-ethyleneimida) and DNA observing reported a reduction in 40% of cell viability. The group of Gao [16] also reported an increase in apoptosis when cell cultures were treated with SWNTs. Monteiro-Riviere et al. in 2005 [17] used MWNTs and reported cell inflammation due to a

overproduction of IL-8. In the same context, Elias et al. [18] reported viability studies of *Entamoeba histolytica* treated with CNx-MWNTs and pure carbon MWNTs showing no toxicity for CNx-MWNTs. Recently, Hirano et al. [19] reported a high toxicity of short MWNTs (67 nm) inducing increase of mRNA levels of some cytokines and disrupt of integrity of the cell membrane. From the above sentences, it is clear that the results regarding the interactions of carbon nanotubes and cells are diverse and sometimes contradictory; this may be due to changes in morphology, synthesis process, functionalization methods and doping differences among the different nanotube samples.

Recently Poland et al. [20] published a controversial paper regarding the carcinogenic activity of asbestos and MWCNTs. These authors emphasize the importance of nanotubes length. This paper has therefore triggered a large number of comments about the danger and use of MWCNTs. For these reasons, it is important to know the precise type of nanotubes were used, the growth conditions, the surface (or functional) groups and the metallic catalyst and dose.

Despite to the number of publications there are only a few reports dealing with the interaction of Nitrogen-doped or Carboxyl functionalized MWCNTs with biological systems. Therefore, it is important to study these novel nanotube system and its bio-response.

## Materials and methods

HEK 293, HeLa and CaSki culture cells were used to study the interaction of cells with different types of CNTs. The cultures were maintained in DMEM, the

medium was periodically changed; this process renews nutrients and avoids the agglomeration of harmful products with the consequent cell death. The protocol for preparing and medium change is explained in appendix A.

For flow cytometry analysis of DNA content it is necessary to label the nucleus with an appropriate fluorescent material. We used propidium iodide; this is a carcinogenic material and must be handled with extreme precaution. Other substances used for flow cytometry preparation is PBS 1x pH 7.2, to wash the samples, trypsin and DMEM. The protocol and reagent preparation is described in appendix B.

For Scanning Transmission Electron Microscopy (STEM) it is necessary to prepare the cells for microscopy studies. The cells must be preserved in a motionless state. In order to achieve this it is essential to clean the samples with PBS; 2% of glutaraldehyde in PBS as a fixing agent; 1% of Osmium tetroxide in PBS as contrast agent; double deionized water to remove salts; ethanol to remove lipids; propylene oxide as polymerize agent, and EPON resin to embed the samples in order to cut them in very thin slices (60 nm thickness). The steps describing the detailed samples preparation appear in appendix C.

## Experimental design

CNTs were sterilized in autoclave and dispersed in DMEM using different concentrations (1, 5 and 10  $\mu\text{g ml}^{-1}$ ). In order to achieve a relatively good dispersion, the samples were ultrasonicated (Ultrasonic Processor, Cole Parmer, Model CPX500) for 15 min, and stored at 4°C prior to use. The crystallinity of f-

COx-MWNT is better when compared to f-CNx-MWNT and f-MWNT. Since highly crystalline nanotubes experience strong van der Waals interactions, these tubes tend to agglomerate faster into bundles. For this reason it was necessary to stir manually the suspensions before each application.

HEK, HeLa and CaSki cells were incubated in a controlled 5% CO<sub>2</sub> atmosphere at 36.5°C, the medium was changed periodically until the cells reach a population of approximately one million per experiment. The experiments that we have carried out are indicated in Table 3.1, and were always repeated twice.

**Table 3.1.** Treatments made to HeLa, CaSki and HEK cells with three types of CNTs. We used cells without treatment as viability control. These conditions are depicted in the first row.

Treatment	concentration (µg/ml)	2 hrs	6 hrs	12 hrs	18 hrs	24 hrs
Control	0	0	0	0	0	0
f-CNx-MWNT	5	5	5	5	5	5
	10	10	10	10	10	10
	5	1	1	1	1	1
f-COx-MWNT	5	5	5	5	5	5
	10	10	10	10	10	10
	5	1	1	1	1	1
f-MWNT	5	5	5	5	5	5
	10	10	10	10	10	10
	5	1	1	1	1	1

Once the cells reached an appropriate count (e.g. one million) the sterile and dispersed nanotubes were added at different concentrations. The samples were stored under controlled environment until they were characterized. For flow cytometry, samples were taken at 2, 6, 12, 18 and 24 hours, and for STEM studies, the samples were incubated for 1.5 hours.

# Characterization

## Flow cytometry

Flow cytometry is a powerful technique able to carry out the analysis of cellular cycle and is used in general for the analysis of multiple parameters of individual cells within heterogeneous populations. The flow cytometer performs this analysis by passing thousands of cells per second through a laser beam and capturing the light that emerges from each cell as it passes through. The gathered data can be analyzed statistically using software that reports the cellular characteristics such as size, complexity, and phenotype. The flow cytometry instrument (Figure 3.1) consists of a fluid system, lasers, an optics system, detectors and the electronic and peripheral computer system. The point where the laser beam and the sample intersect is named interrogation point. At this point, the optics collects the resulting forward scatter, side scatter and fluorescence from the sample.

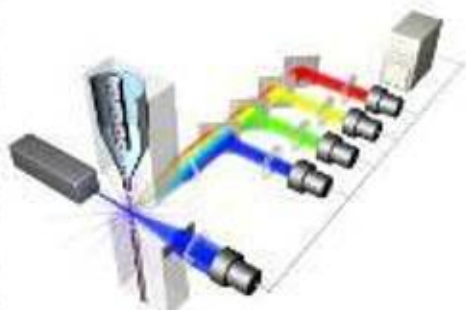


**Figure 3.1** Flow cytometry system. Cell flow is done as a laminar flow, where only a single cell passes through interrogation point. Scatter light is transported and saved by an optic system. Image taken from [antitoga.com](http://antitoga.com).

When a cell passes through the laser, it will refract or scatter light in all angles. Forward scatter is the amount of light that is scattered in the forward direction when a laser light strikes the cell; and the magnitude of forward scatter is proportional to the size of the cell. The flow cytometer apparatus is able to collect light at 90 degrees, named side scatter or light scattered at larger angles. The side scatter light is collected by an array of dichroic glasses, and depending on its wavelength, the light is addressed to different sensors. Side scatter light give us information of granularity, this means that if a cell contains many organelles the amplitude of the signal will be high, but if the cell is simple (has few organelles) the side scatter amplitude will be low.

The light scattered is quantified by a detector which converts intensity into voltage. The scattered light collected by the detector is translated into a voltage pulse, due to that, small cells produce a small amounts of forward scatter and large cells produce large amount of forward scatter, the magitude of the voltage pulse recorded for each cell is proportional to the cell size.

In order to study the cell proliferation using flow cytometry it is necessary to use fluorescent molecules such as propidium iodide (PI) interlayered in the DNA molecules, in order to know indirectly the size of DNA. The flow cytometer have a wavelength detector, which can be tuned to sense the fluorescence emission of PI (the fluorescence excitation maximum is shifted  $\sim 30\text{--}40$  nm to the red and the fluorescence emission maximum is shifted  $\sim 15$  nm to the blue).

In order to achieve the binding between PI molecules and DNA, it is necessary to prepare a staining buffer capable to reach and penetrate the nucleus, it have to

make fluorescent the DNA molecules and destroy undesirable elements (RNA), so this buffer must contain:

1. propidium iodide as fluorescent agent
2. a detergent, this will make all the lipids soluble, destroying the cell membrane. The nucleus membrane is more resistant, so it is not destroyed by the detergent, only small holes in the nucleus membrane are made, these holes enables the cross of PI molecules.
3. an enzyme that digest RNA (RNase). The nucleic acids are made by RNA and DNA, PI also binds to RNA, so it is essential to eradicate the presence of RNA.

We have interest in cell proliferation and apoptosis index. As explained in chapter 1 the DNA size is related to the phase of the cell cycle: G0 and G1 have the same DNA quantity, this DNA starts to grow in synthesis phase until it reaches the double of DNA, it is in G2 phase, is here when mitosis is developed. So, the signal intensity of PI collected by the flow cytometer is proportional to the quantity of DNA in a nucleus, and this intensity tells us about the cell phase. In apoptosis the DNase cut the DNA in small pieces, in this way an apoptotic cell has a fragmented DNA. Some of these small fragments can cross the nucleus membrane and are lost in the processes of washing. Thanks to this loss process we can search for nucleus with fewer quantity of DNA, corresponding to apoptotic cells. Figure 3.2 represents percentage of apoptotic cells and cells in different stages of cell cycle, each phase is enclosed by a cursor, this cursor counts the number of cells in each stage.

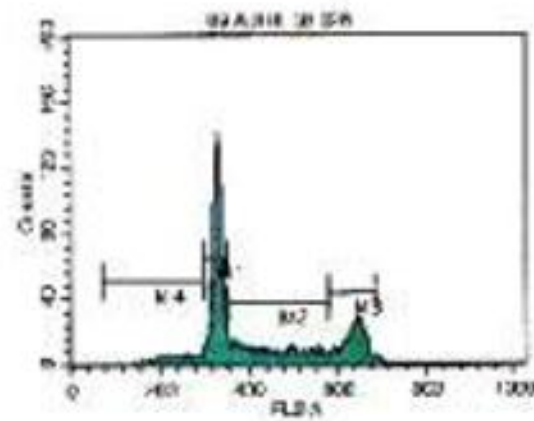


Figure 3.2 Typical scatter pattern of flow cytometry. Are plotted fluorescence versus counts. The M4 zone corresponds to apoptotic cells, M1 to cells in G0 or G1 phase, M2 cells in synthesis phase and M3 represents the number of cells in mitosis or G2 phase.

## Scanning-Transmission Electron Microscopy (STEM)

In order to study the interaction between cells and CNTs, is important to determine how CNTs penetrate the cell membrane and deposits into cytoplasm or other organelles. Therefore, it is necessary to prepare the cells adequately so that they can be studied inside electron microscope chamber.

It is very important to leave intact the cells and study their interactions with the different types of nanotubes. Thus, the specimens need to be stable under TEM examination or STEM environment. There are some considerations for sample preparation: high vacuum, damage from intense electron beam, size of specimen, depth of electron penetration and sample support. The main steps for sample preparation are the following [21]:

1. **Stabilization.** The *Fixation* process prepares the cell for a whole series of traumatic events caused by the electron microscope. The reagent



selected as a fixation agent should transform the protoplasm into stable elastic gelatin. Simultaneously, the spatial relationship of all organelles must be maintained; the phospholipids, which form the framework of the cell, should also be stabilized. *Dehydration* is the complete removal and replacement of all water in the sample with a solvent which is miscible with the embedding medium. Ethanol is commonly used as organic dehydrating agent. Shrinkage, commonly associated with dehydration, can be minimized when using ethanol in increasing concentrations. Finally, some embedding medium are not or only partially miscible in either alcohol or acetone. For this reason, it is necessary the introduction of an intermediate transition solvent which is miscible in both, the dehydrating agent and the embedding medium. The most frequently used transition solvent is propylene oxide with alcohols. *Embedding* includes the gradual removal of the dehydrating agent or transitional solvent and the infiltration of the cell by a resin monomer. The monomer selected should be of low viscosity so that a rapid and homogeneous infiltration takes place. The resin should also be chemically inert with respect to the cells and miscible with the dehydrating agent or the transition solvent. The polymer catalyst should produce uniform polymerization without causing translocation of cellular components. Finally, the resin should also be highly electron transparent and stable under the electron beam for TEM and STEM studies.

2. **Surface preparation.** Once the cells are embedded in the polymer, it is necessary to cut the material for TEM characterization into very thin slices (<100 nm). The best shape for the knife, when cutting, is a

trapezoid, see Figure 3.3. The trapezoid shape should be oriented in the microtome chuck so that the longest parallel side faces down.



**Figure 3.3.** Embedded cells into epoxy resin. Figure a shows the capsule-mold having a trapezoidal shape on the tip. In figures b and c we can observe the trapezoidal shape. Arrows indicate the cellular sample located close to the tip of the capsule.

3. **Mounting the specimen on the grid.** When the samples are cut are deposited onto water surface, and by optical microscopy they are selected and placed on TEM and STEM grids.
4. **Staining.** In order to obtain contrast in the cells and the polymer the samples are stained before they are dehydrated and after mounting them on the TEM grid. Since the main element contained in the cells are carbon, hydrogen, oxygen and nitrogen, the differences in atomic weight are small, heavier elements need to be added for obtaining electron microscopy contrast. In this context, Osmium tetroxide ( $\text{OsO}_4$ ), is the most commonly used fixation agent for electron microscopy studies [22]. The use of this compound is based on two effects: an excellent cellular preservative and a heavy metal capable of

scatter electrons.  $\text{OsO}_4$  can be used as a primary fixation agent or as a post-fixative compound following glutaraldehyde fixation.  $\text{OsO}_4$  is a yellow crystalline material and it should be handled with extreme caution. Since the presence of a gelatin layer on the specimen reduces the contrast of the image, strong staining is necessary. A solution of 1% Uranyl Acetate with absolute ethanol provides good results when the process occurs in 10-45 min.

## Results & Discussion

### Flow cytometry - Fluorescence-activated cell sorting

The cells were treated with CNTs and placed in cell culture plates (48 wells). Cells were incubated and monitored at 2, 6, 12, 18 and 24 hours. Then cells were prepared for FACS, after treated them with PI.

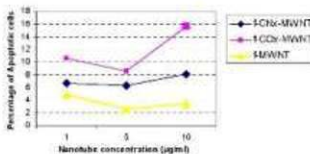
#### **Nanotube interaction with HEK Cells**

Table 3.2 displays data related to the percentage of apoptotic HEK cells and different treatments of carbon nanotubes. The control row represents no CNT treatment cells, and the measurements were obtained at 2, 6, 12, 18 and 24 hours. The columns in Table 3.2 indicate the percentage of apoptotic cells for each nanotube type and for different nanotube concentration in solution. The higher apoptosis percentage (colored in red) depend on the concentration, time. The percentages colored in blue correspond to the lower percentages observed in the study with these cells.

**Table 3.2.** Percentage of apoptotic HEK cells treated with different types of CNTs in relation to the control.

Treatment	Concentration ( $\mu\text{g ml}^{-1}$ )	Percentage of Apoptotic cells for each time sample:				
		2 hours	4 hours	12 hours	18 Hours	24 hours
control	-	13.03	4.00	5.26	8.11	13.80
	1	14.46	6.72	6.95	9.59	12.00
	5	16.06	6.29	4.90	5.37	14.17
f-CNs-MWNT	10	16.73	8.11	6.68	7.66	12.83
	1	17.02	10.55	5.45	8.36	18.50
	5	19.63	8.84	5.36	7.90	16.18
f-CDs-MWNT	10	14.87	15.94	4.08	5.18	17.16
	1	15.67	6.91	2.19	8.26	17.08
	5	15.16	2.60	5.38	6.68	16.43
f-MWNT	10	14.21	3.47	4.87	5.77	19.40

Figure 3.4 is a plot of apoptotic cells versus f-CNT concentration, after 6 hours of initiating the treatment. At this time, the apoptotic cells in the control sample is 4% (see Table 3.2). In Figure 3.4 is also plotted the percentage of apoptotic cells versus time using concentration of 5 and 10  $\mu\text{g ml}^{-1}$



**Figure 3.4** Apoptotic cells treated with different concentrations of 3 types of CNTs after 6 hours of initiating the treatment.

In Figure 3.5 one could observe that the tendency of apoptosis decreases because the cells remains duplicating after the nanotubes where introduced. The level of apoptosis observed for the first hours is possibly due to the instantaneous stress caused by nanotubes. It can be observed that the higher apoptosis index takes place after 2 hours for  $f\text{-CNx-MWNTs}$  and for  $f\text{-COx-MWNTs}$ . It is noteworthy that  $f\text{-COx-MWNTs}$  always show a higher apoptosis when the concentration of  $5 \mu\text{g ml}^{-1}$  is used. However  $f\text{-MWNTs}$  induce the lower apoptosis percentage for the first hours and  $f\text{-CNx-MWNTs}$  exhibit the lower apoptosis percentage for later hours.

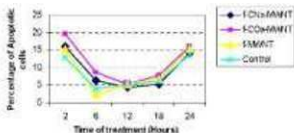


Figure 3.5 Represents percentage of apoptotic cells treated with different types of CNTs plotted against time. Nanotubes concentration is fixed to  $5 \mu\text{g ml}^{-1}$ . Light blue line represents control sample without CNTs treatment.

### Interaction of HeLa cells and Nanotubes

The cell cycle of HeLa cells was monitored when treated with the different types of nanotubes at different doses. These results are shown in Table 3.3, and there are not data of complete cell cycle at 2 and 6 hours.

**Table 3.3.** Percentages of HeLa cells in different phases of the cell cycle when treated with three different types of CNTs at different doses.

Treat exposure	Treatment	Concentration (µg/ml)	G0/G1	S	G2/M	Apoptosis	
2 hrs	Control	-	-	-	-	9.81	
	ACN-MWNT	1	-	-	-	9.78	
		5	-	-	-	10.00	
		10	-	-	-	11.58	
	ACN-MWNT	1	-	-	-	13.14	
		5	-	-	-	-	
		10	-	-	-	5.23	
	MWNT	1	-	-	-	7.63	
		5	-	-	-	11.44	
		10	-	-	-	9.93	
	4 hrs	Control	-	-	-	-	9.79
		ACN-MWNT	1	-	-	-	9.90
5			-	-	-	9.46	
10			-	-	-	9.99	
ACN-MWNT		1	-	-	-	10.15	
		5	-	-	-	11.42	
		10	-	-	-	14.90	
MWNT		1	-	-	-	9.57	
		5	-	-	-	7.08	
		10	-	-	-	9.43	
12 hrs		Control	-	49.11	29.87	19.97	12.01
		ACN-MWNT	1	-	-	-	-
	5		49.90	29.86	11.06	14.21	
	10		44.12	29.43	10.36	20.50	
	ACN-MWNT	1	52.94	26.55	10.05	10.19	
		5	48.00	29.43	10.31	12.12	
		10	43.32	31.24	11.30	14.64	
	MWNT	1	48.13	29.89	12.19	10.79	
		5	46.58	30.72	8.41	14.71	
		10	44.76	32.28	8.20	13.76	
	18 hrs	Control	-	50.73	37.06	19.25	2.99
		ACN-MWNT	1	51.09	31.36	13.91	4.37
5			46.57	31.34	12.90	8.22	
10			39.01	39.36	16.79	7.03	
ACN-MWNT		1	49.15	33.59	14.00	3.49	
		5	51.07	32.55	17.49	3.79	
		10	49.22	32.21	13.50	9.07	
MWNT		1	47.57	32.76	13.39	6.09	
		5	48.47	33.70	12.61	9.35	
		10	49.12	34.99	13.01	5.49	
24 hrs		Control	-	49.83	34.82	15.20	5.67
		ACN-MWNT	1	49.00	36.80	8.85	8.85
	5		41.44	34.20	14.00	10.60	
	10		36.64	34.71	13.15	16.70	
	ACN-MWNT	1	47.50	38.45	16.10	5.75	
		5	39.34	33.26	19.39	10.50	
		10	37.25	33.25	17.09	21.58	
	MWNT	1	28.57	39.29	12.20	21.50	
		5	-	-	-	-	
		10	-	-	-	-	

There are not only remarkable differences between the responses of different CNTs, but also the apoptosis percentage increases significantly, Figure 3.6 A shows the same tendency to decrease and then increase the percentage of apoptosis. This may be due because mitosis process began before the CNTs affected the cells. We can also observe that there are not remarkable differences in percentage of mitotic cells, but the cell growth percentage decreases, see Figure 3.6 C and D. Here we could see that CNTs not only could affect the cell viability, but also affect the whole cell cycle.

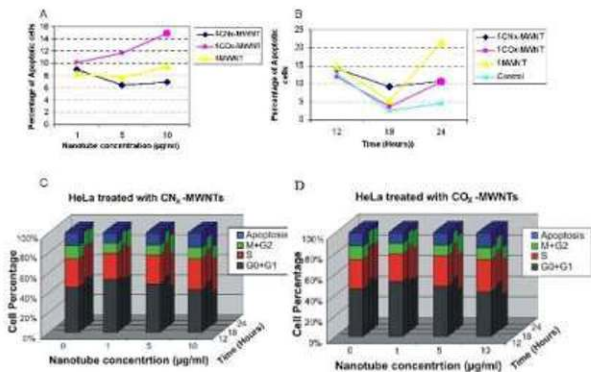


**Figure 3.6.** A and B correspond to plots relating the apoptotic cells against CNTs concentration and time respectively; C and D depict the percentage of the whole cell cycle (mitosis, synthesis, growth phases and apoptosis) versus CNTs concentration and time.

### **Interaction of CaSki Cells and different types of Nanotubes**

Treatment with CaSki cells was almost identical to the treatment observed for the HeLa cells. In this context Table 3.4 shows all data corresponding to the cell cycle of CaSki cells and the CNTs interaction.

Here, we can observe a clear tendency to increase the apoptotic percentage when the CNTs concentration is increased. Apparently, *f*-CO<sub>x</sub>-MWN<sub>T</sub>s induce low level of apoptosis as the CNTs concentration increases, but the three different types of CNTs increase the apoptosis percentage as their concentration increase, Figure 3.7 A.

These cells exhibited higher levels of apoptosis after 24 hours of treatment, and the same phenomena observed in HeLa cells was present with the CaSki cells. The presence of high levels of apoptosis for the first hour, followed of a minimum and then increases reaching the maximum after 24 hours, see Figure 3.7 B.



**Table 3.4.** Percentages of CaSki cells in different phases of the cell cycle when treated with these different types CNTs at different doses

Time exposure	Treatment	Concentration ( $\mu\text{g/ml}$ )	G0-G1	S	M-G2	Apoptosis	
2 hrs	Control	-	-	-	-	5.47	
	FCNs-MWNT	5	-	-	-	10.9	
		5	-	-	-	10.99	
		10	-	-	-	13.47	
	FCOs-MWNT	5	-	-	-	12.64	
		5	-	-	-	14.508	
		10	-	-	-	4.796	
	MWNT	5	-	-	-	6.09	
		5	-	-	-	8.006	
		10	-	-	-	4.495	
	8 hrs	Control	-	-	-	-	7.99
		FCNs-MWNT	5	-	-	-	13.36
5			-	-	-	15.72	
10			-	-	-	19.374	
FCOs-MWNT		5	-	-	-	1.26	
		5	-	-	-	4.415	
		10	-	-	-	3.006	
MWNT		5	-	-	-	4.406	
		5	-	-	-	18.198	
		10	-	-	-	7.43	
12 hrs		Control	-	54.265	26.13	23.07	0.43
		FCNs-MWNT	5	57.82	24.43	18.50	1.31
	5		56.96	25.36	8.815	8.006	
	10		46.34	37.81	8.08	18.80	
	FCOs-MWNT	5	64.926	23.36	9.95	2.690	
		5	57.465	24.875	12.249	5.81	
		10	51.796	21.796	7.390	15.70	
	MWNT	5	64.265	25.25	8.655	1.81	
		5	60.366	25.48	8.485	6.06	
		10	58.1	25.05	8.2	8.97	
	18 hrs	Control	-	62.16	24.528	13.29	0.49
		FCNs-MWNT	5	60.986	26.21	8.8	3.22
5			57.8	21.67	11.61	8.030	
10			58.806	18.21	11.36	14.835	
FCOs-MWNT		5	71.43	8.936	17.18	2.836	
		5	75.47	6.7	15.8	2.15	
		10	59.065	22.21	13.475	5.83	
MWNT		5	61.786	25.58	12.24	1.096	
		5	63.026	31.18	10.988	1.996	
		10	60	24.82	8.48	15.7	
24 hrs		Control	-	66.37	29.895	6.21	2.096
		FCNs-MWNT	5	54.36	28.896	10.11	5.62
	5		62.82	34.84	6.42	14.29	
	10		49.24	31.21	8.880	21.41	
	FCOs-MWNT	5	69.925	14.375	5.02	5.196	
		5	73.37	8.82	12.93	4.8	
		10	51.926	27.81	8.885	8.86	
	MWNT	5	58.22	30.83	6.78	2.816	
		5	58.356	25.58	6.78	9.13	
		10	36.1	23.73	3.995	34.02	

Figure 3.7 C and D plot  $f_{\text{CNx-MWNTs}}$  and  $f_{\text{COx-MWNTs}}$  respectively. The CaSki cell cycle was affected in different ways depending on the CNT type. For example  $f_{\text{CNx-MWNTs}}$  induces an increment on mitotic cell percentage as the concentration increases. In contrast,  $f_{\text{COx-MWNT}}$  and  $f_{\text{MWNT}}$  induce a decrease on the mitotic cell percentage. The synthesis percentage remains stable without important changes, and the percentage of cells growing always decreases as the CNTs concentration increases. Also note that apoptosis tends to increase in time for all conditions.

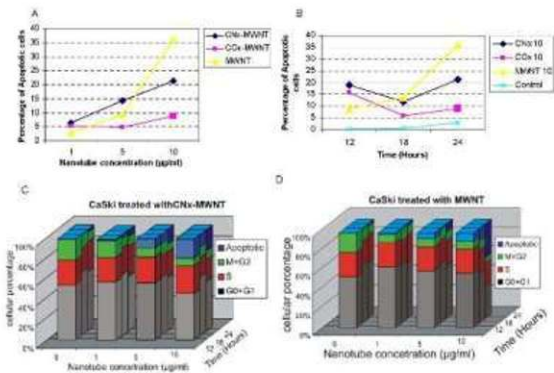


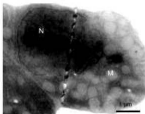
Figure 3.7. A and B plot percentage of apoptotic cells against the CNTs concentration and time respectively; C and D plot percentage of the whole cell cycle (mitosis, synthesis, growth phases and apoptosis) against CNTs concentration and time.

## Scanning-Transmission Electron Microscopy (STEM)

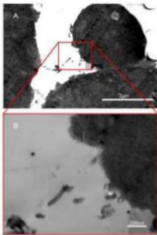
All cells were incubated in a controlled atmosphere of 5% of CO<sub>2</sub> at 36.5°C and the medium was changed periodically. For this characterization only small amounts of cells have a visible small bottom in Eppendorf tubes. Cells were incubated for 1.5 hours after the CNT treatment, then the medium was removed and samples were washed with PBS and then proceeded with the preparation for electron microscopy studies (Appendix C for details)

### HEK Cells and Nanotubes

In Figure 3.8 a healthy HEK cell is observed; the bigger organelle is the nucleus with an average diameter of 3µm and the mitochondria of 450nm in diameter. Note that the length of the cell is ca. 6.5µm.

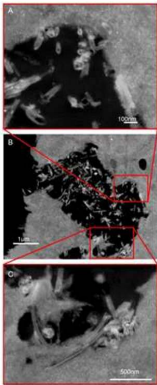


**Figure 3.4** A healthy HEK cell, previously treated for electron microscopy. The line crossing the cell is due to irregularities of the diamond blade. M= mitochondrion, N=Nucleus.



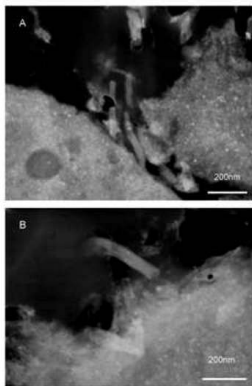
**Figure 3.9.** Ultrathin section of HEK cells treated with *jCNx-MWNTs*. After incubation, the cells were fixed, stained, dehydrated, and embedded in EPON 812 resin. Ultrathin layers (60 nm thick) were cut with an ultramicrotome. A) The entire cell; B) a subsequent magnifications of *jCNx-MWNT* crossing the cell membrane. Nanotube concentration correspond to  $10 \mu\text{g ml}^{-1}$

Figure 3.9 A shows a group of HEK cells treated with *jCNx-MWNTs*. Figure 3.9 B, reveals some CNTs penetrating onto the membrane surface, CNTs exhibit an average diameter of 40nm and the length of the crossing nanotube corresponds to 220 nm.



**Figure 3.10** HEK cells prepared for electron microscopy studies. A shows some *f*CN<sub>x</sub>-MWNTs penetrating the cell membrane. In B some CNTs are surrounded by HEK cells. It is noteworthy that these cells do not exhibit a typical round morphology, in contrast linear edges are present. C shows how CNTs are placed in the cell membrane. Nanotube concentration correspond to 10 µg ml<sup>-1</sup>

Some of the cells were affected morphologically adopting uncommon shapes. It seems that CNTs work as template. Detailed magnification shows some CNTs crossing the cell membrane. Figure 3.6 C reveals how a nanotube deforms the cell membrane, apparently the cell is not in apoptosis.



**Figure 3.11.** STEM images of HEK cells treated with *fCOx*-MWNTs. In A some nanotubes are close to the cell membrane, and in B some CNTs are crossing the cell membrane. Nanotube concentration correspond to  $10 \mu\text{g ml}^{-1}$

*f*-COx-MWNTs presented a higher index in apoptotic cells. In Figure 3.11 A some nanotubes in the periphery of the cell are observed. Higher magnifications indicate these nanotubes crosses cell membrane causing no cellular death (see image 3.11 B). Although *f*-MWNTs showed the lower apoptosis index and *f*-CNx-MWNTs deform the cells morphology, these effects were not observed in cells treated with *f*-COx-MWNT or *f*-MWNT.

### HeLa Cells and Nanotubes

HeLa cells were treated in the same way as the HEK cells. Here, these cells presented more problems when a medium change was required; it was necessary to let them stay for 10 minutes with trypsin in order to take apart the cells from the flask. Figure 3.12 shows a normal HeLa cell, this cell has a diameter of 13.5  $\mu\text{m}$ , and the nucleus has a minimum diameter of 8  $\mu\text{m}$  and a maximum of 11  $\mu\text{m}$ .

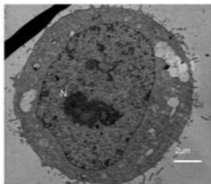


**Fig 3.12** STEM image of an ultrathin slice of a HeLa cell without CNT treatment. The cell culture was fixed, dehydrated, stained and embedded with EPON, slices were then cut with an ultramicrotome (60 nm). N= nucleus



**Figure 3.13** STEM image of HeLa cells treated with *f*COx-MWNT. Some nanotubes in figure A cross the cell membrane and nucleus. In B it appears that the cell phagocytoses CNTs, thus avoiding cell damage. Nanotube concentration correspond to  $10 \mu\text{g ml}^{-1}$

The uptake of CNTs was similar for the three different types, no cell damage was observed when they cross the cell membrane. In Figure 3.13 we observed how *f*-COx-MWNT can penetrate the membrane (Figure 3.13 A and B) and some nanotubes reach the nucleus (Figure 3.13 A). In other case some nanotubes penetrate into the membrane without notable cell damage (see Figure 3.13 B).

Figure 3.14 depicts two apoptotic HeLa cells treated with *f*-MWNTs. In this case we found more apoptotic cells than in other cases, according to Flow cytometer data. In Figure 3.14 A, the cell is in an advanced apoptotic state, the whole nucleus is fragmented in apoptotic bodies; and the membrane starts to collapse.



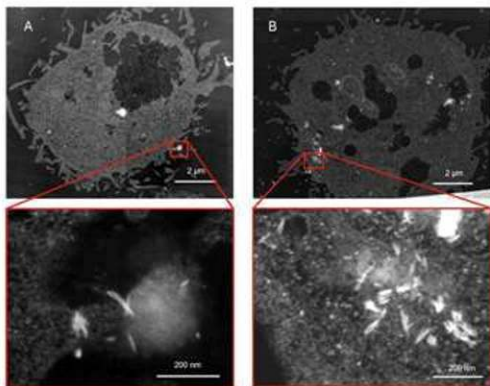


**Figure 3.14** STEM image of HeLa cells treated with *f*MWNTs. These cells are in an apoptotic phase, magnifications shows nanotubes crossing cell membranes, Nanotube concentration correspond to  $10 \mu\text{g ml}^{-2}$

Higher magnifications of the images shows that CNTs do not damage the cell membranes, *f*CNTs are not located in any specific organelle. In Figure 3.14 B it is possible to observe more nanotubes dispersed in the cytoplasm.

### CaSki Cells and nanotubes

Figure 3.15 shows a healthy CaSki Cell in mitosis phase. We did not face problems for sample preparation, and we found a major quantity of mitotic CaSki cells when compared to the HeLa cells.

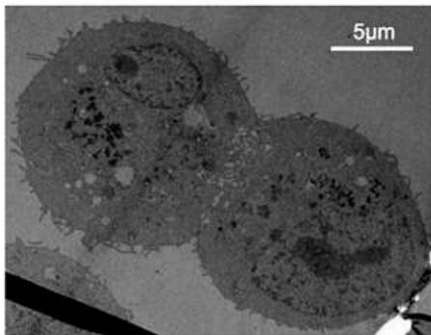


**Figure 3.15.** STEM image of CaSki cell in mitosis embedded in epoxy resin EPON. The cells were previously fixed and stained. Samples are cut in thin slices of 60nm with an ultramicrotome. The image shows clearly some organelles and both nucleus.

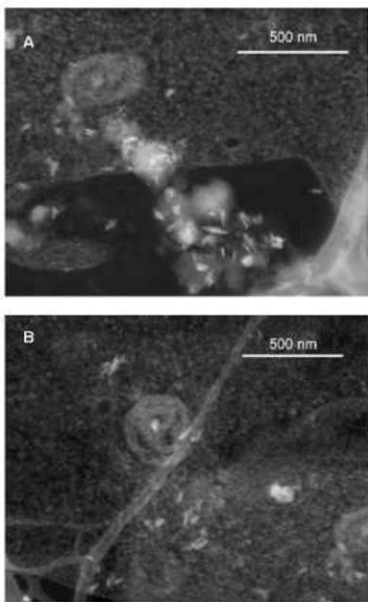
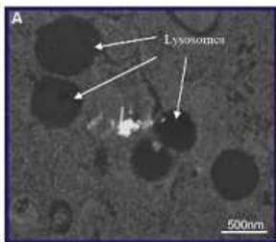
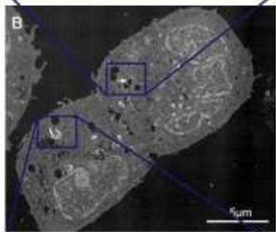


**Figure 3.16.** TEM image of CaSki cells treated with fCOs-MWNT. In A are some nanotubes crossing cell membrane appear, and in B shows apparently CNTs can be observed in the mitochondria and some others in the cytoplasm. Nanotubes concentration correspond to 10  $\mu\text{g mL}^{-1}$ .



*fCOx-MWNTs* interacting with CaSki cells are illustrated in Figure 3.16. Here one can see how CNTs cross the cell membrane. In B some nanotubes are found inside the mitochondrion.



*fCNx-MWNTs* can also be seen in Figures 3.17 interacting with a mitotic CaSki cell. Higher magnification images reveal that nanotubes are immersed in the cytoplasm almost in contact with lysosome.

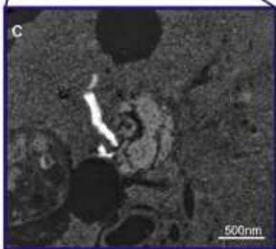


**Figure 3.17.** STEM images of CaSki cells treated with *fCNx-MWNTs*. A shows a cell in mitosis stage and a few mitotubes can be clearly seen B displays a healthy cell. Nanotubes concentration corresponded to 10 µg/ml<sup>2</sup>

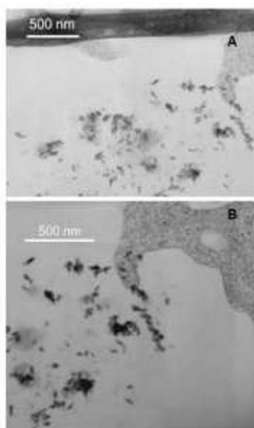


**Figure 3.18.** STM images of CaSki cells treated with f-MWNTs. In figure A some nanotubes reach the nucleus and can be observed at higher magnifications. In B some nanotubes crossing the cell membrane appear and no damage was caused to the cells. Nanotubes concentration correspond to 10  $\mu$ g/ml

Figure 3.18 displays some CNTs into cell, some nanotubes reaches the nucleus, the higher apoptosis index was induced by f-MWNT.

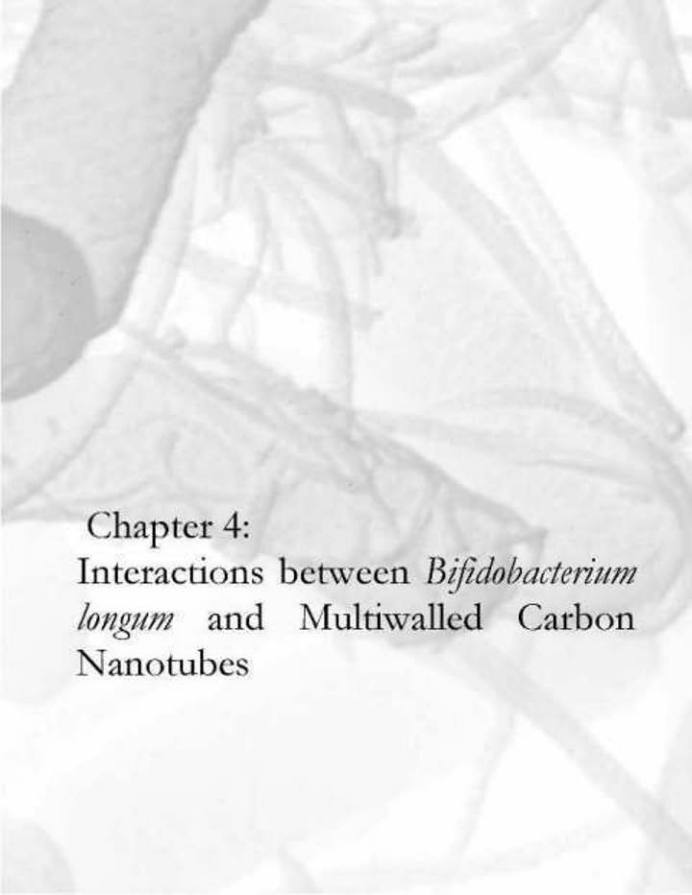
## References

- [1] Partillo, R. A., Husa, R. O., Story, M. T., Ruckert, A. C., Shalaby, M. R., Mattingly, R. F., Tumor antigen and human chorionic gonadotropin in CaSki cells: a new epidermoidcervical cancer cell line. *Science* 24 June 1977 196:1456-1458.
- [2] Graham, F. L., Smiley, J., Russell, W.C., Nairn, R. Characteristics of a human cell line transformed by DNA from human adenovirus type 5. *J. Gen. Virol* 2005 36 (1): 59-74.
- [3] Bianco, A., Wu, W., Pastorin, G., Klumpp, C., Lacerda, L., Partidos, C. D., Kostarelos, K., Prato, M., *Nanotechnologies for the Life Sciences* Vol 10 Nanomaterials for Medical Diagnosis and Therapy, Chapter 3 Carbon Nanotube-based Vectors for Delivering Immunotherapeutics and Drugs, pag 85, Edit. Challa S. S. R. Kumar, Wiley-Vch.
- [4] Jin, G., Wang, H., Yan, L., Wang, X., Pei, R., Yan, T., Zhao, Y., Guo, X. Cytotoxicity of single-wall nanotube, multi-wall nanotube and fullerene, *Environ. Sci. Technol.* (2005) 39,1378-1383.
- [5] Manna, S. K., Sarkar, S., Barr, J., Wise, K., Barrera, F. V., Jejelowo, O., Rico-Ficht, A. C., Ramesh, G. T., Single-walled carbon nanotube induces oxidative stress and activates nuclear transcription factor-kB in human keratinocytes, *Nano Lett.* (2005) 5 1676-1684.
- [6] Bottin, M., Bruckner, S., Nika, K., Bottin, N., Belluci, S., Magrini, A., Bergamaschi, A., Mustelin, T. Multi-walled carbon nanotubes induce T lymphocyte apoptosis. *Toxicol. Lett.* (2006) Jan 5; 160, 2, 121-126.
- [7] Shvedova, A. A., Kisin, E. R., Murray, A. R., Gandelsman, V. Z., Maynard, A. D., Baron, P. A., Castranova, V. Exposure to carbon nanotube materials:

- assessment of nanotube toxicity using human keratinocytes cells, *J. Toxicol. Environ. Health A* (2003), 66, 1909-1926.
- [8] Sayes, C. M., Liang, F., Hudson, J. L., Mendez, J., Guo, W., Beach, J. M., Moore, V. C., Doyle, C. D., West, J. L., Billups, W. E., Ausman, K. D., Colvin, V. L. Functionalization density dependence of single walled carbon nanotubes cytotoxicity in vitro. *Toxicol Lett.* (2006) 161, 135-142.
- [9] Dumortier, H., Lacotte, S., Pastorini, G., Marega, R., Wu, W., Bouifazi, D., Briand, J. P., Prato, M., Bianco, A. Functionalized carbon nanotubes are non-cytotoxic and preserve the functionality of primary immune cells. *Nano Lett.* (2006) Jul; 6, 7, 1522-1528.
- [10] Sato, Y., Yokoyama, A., Shibata, K., Akimoto, Y., Ogino, S., Nodasaka, Y., Kohgo, T., Taura, K., Akasaka, T., Uo, M., Motomiya, K., Jayadevan, B., Ishiguro, M., Hatakeyama, R., Watari, F., Tohji, K., Influence of length on cytotoxicity of multi-walled carbon nanotubes against human acute monocytic leukemia cell line THP and subcutaneous tissue of rats in vivo. *Mol. Biosyst.* 1005, 1, 176-182.
- [11] Kiura, K., Sato, Y., Yasuda, M., Fugetsu, B., Watari, F., Tohji, K., Shibata, K. Activation of human monocytes and mouse splenocytes by single-walled carbon nanotubes, *J. Biomed. Nanotechnol.* (2005) 1, 359-364.
- [12] Tian, F., Cui, D., Schwartz, H., Estrada, G. G., Kobayashi, H. Cytotoxicity of single-walled carbon nanotubes on human fibroblasts. *Toxicol in vitro* (2006) 20, 7, 1202-1212.
- [13] Pautarotto, D., Briand, J.-P., Prato, M., Bianco, A. Translocation of bioactive peptides across cell membrane by carbon nanotubes, *Chem. Commun.* (2004) 16-17.

- [14] Pantarotto, D., Singh, R., McCarthy, D., Erhardt, M., Briand, J.-P., Prato, M., Kostarelos, K., Bianco, A. Functionalized Carbon nanotubes for plasmid DNA gene delivery, *Angew. Chem. Int. Ed.* (2004) 43,5242-5246.
- [15] Liu, Y., Wu, D. C., Zhang, W. D., Jiang, X., He, C.B., Chung, T. S., Goh, S. H., Leong, K. W. Poly-ethylsuccinimide-grafted multiwalled carbon nanotubes for secure noncovalent immobilization and efficient delivery of DNA, *Angew. Chem. Int. Ed.* (2005) 44, 4782-4785.
- [16] Cui, D., Tim, F., Ozkan, S., Wang, M., Gao, H. Effect of single walled carbon nanotubes on human HIEK293 cells, *Toxicol. Lett.* (2005) 155, 73-85.
- [17] Monteiro-Riviere, N. A., Nemanich, R. J., Inman, A. O., Wang, Y. Y., Riviere, J. F. Multiwalled carbon nanotube interactions with human epidermal keratinocytes, *Toxicol. Lett.* (2005) 155, 377-384.
- [18] Elias, A. L., Carrero-Sanchez, J. C., Terrones, M. H., Endo, M., Lacroette, J. P., Terrones, M. M., Viability Studies of Pure Carbon- and Nitrogen-Doped Nanotubes with *Entamoeba histolytica*: From Amoebicidal to Biocompatible Structures, *Small* 2007, 3, No. 10, 1723-1729.
- [19] Hirano, S., Kanno, S., Furuyama, A., Multi-walled carbon nanotubes injure the plasma membrane of macrophages. *Toxicol. Appl. Pharmacol.* (2008) jul 3.
- [20] Poland, C. A., Duffin, R., Kinloch, I. K., Maynard, A., Wallace, W. A. H., Seaton, A., Stone, V., Brown, S., Macnee, W., Donaldson, W. Carbon nanotubes introduced into the abdominal cavity of mice show asbestos like pathogenicity in a pilot study, nature nanotechnology, *Advance online publication.*
- [21] University of Georgia, laboratory requirements, BIO 50501./70501.
- [22] Palade, G. E., A study of fixation for Electron Microscopy 1952, *J. Exp. Med.* 95, 3, pag 285.



A grayscale micrograph showing a dense network of carbon nanotubes. The nanotubes appear as thin, elongated, and somewhat curved fibers, some of which are bundled together. The background is light and textured, suggesting a substrate or a network of other nanotubes.

Chapter 4:  
Interactions between *Bifidobacterium*  
*longum* and Multiwalled Carbon  
Nanotubes

using the microwave technique helped with MWNTs to introduce genomic material into bacteria.

In this chapter, we used functionalized CNTs to transform genetically *Bifidobacterium longum*, (*B. longum*). The importance of these bacteria is huge, because it represents 95% of the intestinal flora in breast-fed infants and gradually decreases in number from the time of weaning. Beneficial bacteria are represented by *B. longum* and *Lactobacillus* since they inhibit the growth of harmful bacteria and exert many helpful physiological effects such as immunological activation, vitamin synthesis, assistance in digestion and absorption, prevention of colonization of pathogens, improvement of the intestinal flora, inhibition of intestinal putrefactive substances and activation of intestinal conditioning. The main characteristics of *B. longum* are the production of lactic acid and acetic [6]. Furthermore, it has been reported [7] that genetically engineered *B. longum*, after intravenous injection, could locate a wide variety of cancers due to its anaerobiosis predilection. Bandaru et al. [8] reported that lyophilized cultures of *B. longum* induce inhibition effects on liver, mammary and colon cancers, in the same way other groups report inhibition of colon cancer [9] and liver [10].

Bacteria **transformation** is the process by which bacterial cells take DNA molecules. It could be in a plasmidic form, and integrate it to their own DNA, synthesizing the corresponding proteins and duplicating them in each cell division. This process increases biological functions, but unfortunately *B. longum* transformation is not simple due to their membrane thickness, as discussed in chapter one, there are two types of bacteria: Gram positive and Gram negative, the latter are relatively easy to transform, e.g. *E. coli*, but Gram positive bacteria,

such as *B. longum*, possess a thicker membrane, thus making difficult the transformation. There are only a few reports about the successful transformation of *B. longum* [11, 12, 13], but the transformation efficiency rate in these works are below of  $1 \times 10^5$  transformants per  $\mu\text{g}$  of DNA.

The interest of *B. longum* transformation is because it enables novel medical and anticancer treatments, so that drugs for *in situ* delivery could be produced.

## Materials and Methods

### Bacteria Strains and plasmids

The plasmid pRI, containing the chloramphenicol resistance and the synthetic IL-10 gene (Reyes-Escogido et al., 2007) was used. The plasmid was purified from *E. coli* TOP10 strain using the miniprep following the manual instructions (QUIAGEN). The presence of pLR plasmid on *B. longum* was confirmed by amplification of the 490 pb fragment of IL-10 gene using the upstream primer sequence 5'-GAT ATG TCG CXX GGC CAG GGC ACG-3' and the downstream primer sequence 5'-GGA TCC TCA GTT GCG GAT TTT CAT-3'. The PCR mix was as follows: Taq polymerase buffer 10x, MgCl<sub>2</sub> 25 mM, dNTPs 10  $\mu\text{M}$ , forward y reverse oligonucleotids 10 pM/each, and 0.5U Taq polymerase (Invitrogen). One colony was took with a pipet tip and mixed with PCR reaction mix. Amplification was carried out in the iCycler PCR (Bio-Rad). The conditions for replication was 94°C per 10 min. for denaturalization, 35 cycles at 94°C for 1 min, 59°C per 45 sec, 72°C for 2 min. and a final extension of 7 min at 72°C. After the reaction were finished, 10 ml PCR products were

electrophoresed in 1.2% agarose gel, stained with ethidium bromide dye and analyzed with BioRad Gel Doc 2000 system

For Petri dishes we added 1.5% wt. of Bacteriologic Agar to DMEM medium.

The plasmid pLR-hIL-10 [14] was used for transformation, designed at IPiCyT, by Lourdes Reyes during her PhD research, see Figure 4.1.

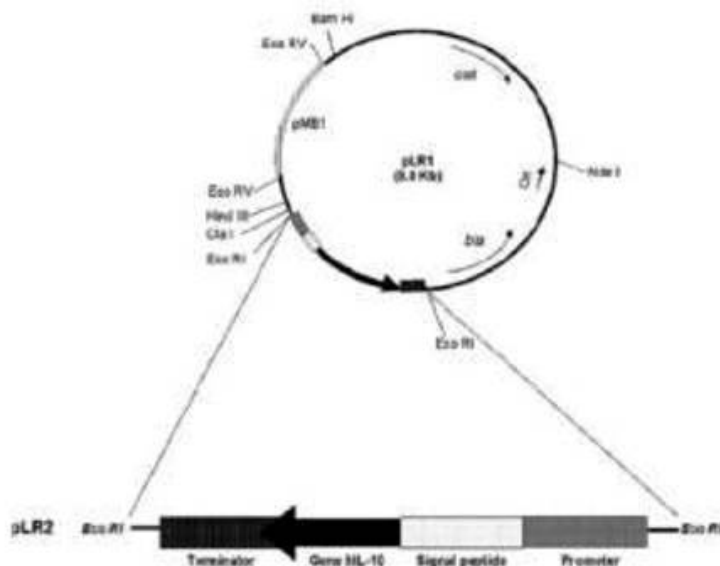


**Figure 4.1** Schematic representation of pLR plasmid. The HU promoter and terminator, the signal peptide BIF3 was fused to the synthetic hIL-10 gene. When the expression cassette was ligated in the sense of bla gene, named as pLR1, contrary to gene bla was named as pLR2 (zoomed image). pMB1 represents the replicon for Bifidobacterium, Ori, E. coli origin, bla, Ampicillin resistance, cat, Chloramphenicol resistance. Taken from [14]

## Microscopy Analysis

Sample preparation, materials and protocols for scanning and transmission electron microscopy are described in Appendix C.

## Experimental Design

Three different types of CNTs were used for *B. longum* transformation: f-MWNTs, f-CN<sub>x</sub>-MWNTs and f-CO<sub>x</sub>-MWNTs.

The CNTs were functionalized in a sulfuric-nitric [3:1] acid solution for 2 and 24 hours, which generated carboxyl, hydroxyl, carbonyl and sulfate groups [17]. The nanotube suspensions were washed once with NaOH 1M and twice with DD H<sub>2</sub>O. The samples were then dried for 24 hours. The functionalized nanotubes were ultrasonicated in for 15 min in order to obtain enhanced dispersions.

Three CNTs types were dispersed in sterile and distilled water with a concentration of 50µg ml<sup>-1</sup>.

Plasmid pLR-hIL-10 gene was used to transform *Bifidobacterium longum* ATCC 15707 strain, using three different types of transformations. *B. longum* was inoculated in 5 ml of MRS (see appendix F) medium with 0.05% cysteine, incubated all night at 37°C. The culture was diluted 1:25 in fresh medium and incubated at 37°C for 3 hours until reaching an approximately optical density

(OD<sub>600</sub>) of 0.3. The culture was then centrifuged at 8000 rpm for 15 minutes at 4°C (Sorvall, Modell Super T21), and the supernatant was discarded. The cell pellet was washed twice in sucrose 0.5 M at 4°C. In cold eppendorf tubes, we mixed 5 µg CNTs, 0.5 µg of Plasmid pLR and 5 µl of competent *B. longum* cells and let for 15 minutes and proceeded with the transformation protocols.

## Transformation

In order to achieve bacterial transformation we used three different methods:

- a) **Electroporation** as described by Arguani et al. [13], is based on applying a high voltage pulse into bacteria, thus weakening the membrane for foreign DNA insertion
- b) **Heat shock** transformation [15], consists of a drastic increase in the initial temperature (from 4°C to 42 °C) of the *B. longum*-DNA-CNTs solution with the subsequent return to a stable temperature (4°C), that enable channels for plasmid incoming through the membrane.
- c) **Microwaves pulse** transformation, proposed by Fregel et al. in January of 2008 [16], consists of increasing the transformation efficiency of *E. coli* using typical Heat shock transformation. The use of Microwave pulse and CNTs was first proposed by Rojas-Chapana et al in 2005 [5] using *E. coli*. The conditions in our experiment were a 115 watts and 2minutes pulse, that corresponds to the lowest microwave power setting.

These three transformation protocols are described in detail in Appendix D.

Bacteria were then recovered in fresh MRS medium without antibiotic. Subsequently they were diluted at 1:1000000 and plated in MRS-Agar containing  $10\mu\text{g ml}^{-1}$  Chloramphenicol, and stored at  $37^{\circ}\text{C}$  for 3 to 5 days.

## Characterization

The oxidation treatment in acid solution for 2 and 24 hours result in different lengths of the nanotubes. We measured the nanotube lengths from SEM micrographs and then carried out a statistic analysis.

Colonies were counted in order to determine the transformation efficiency.

In order to visualize the interaction between CNTs and *B. longum* we carried out SEM and STM. The preparation for STEM or TEM was the same used in human cells (see previous chapter). Bacteria preparation for SEM was similar, but the protocol is stopped before the addition of propylene oxide; the samples in alcohol are dropped on a silicon substrate and let them at room temperature until the solvent evaporates.

To confirm the insertion of pLR-hIL10 plasmid into *B. longum*, plasmid transformants were obtained and the IL-10 fragment was amplified by the PCR technique, using a thermocycler (Bio-Rad, Thermocycler, mod. 382BR). Figure 4.2 shows a time versus temperature diagram used for the PCR.

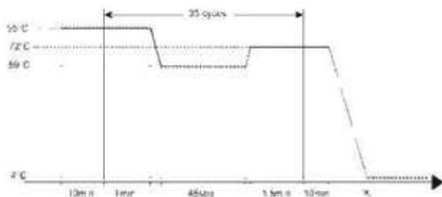


Figure 4.2 Time versus temperature diagram PCR for hIL-10.

## Results and Discussion

Different types and sizes of CNTs are illustrated in Figure 4.5. The length statistic graphs are plotted below each CNT type, and we can see a decrease in length when CNTs are treated for 24 hours in comparison with the 2 hour treatment. The images were selected in zones showing a good dispersion and a wide variety of CNTs lengths.



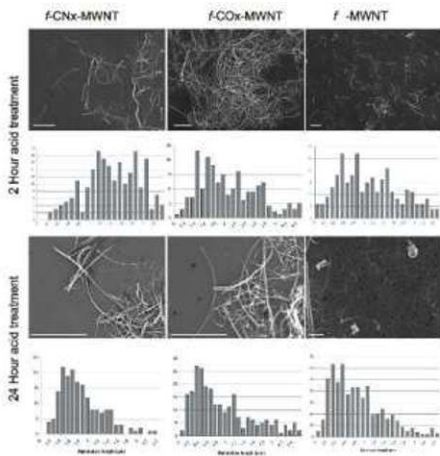


Fig. 4.3. SEM image of  $fCNx$ -MWNT,  $fCOx$ -MWNT and  $f$ -MWNT treated in acid for 2 and 24 hours. Size distribution shows an average length of the nanotubes treated for 2 hours in acid:  $1.5\mu m$  for  $fCNx$ -MWNT,  $1.8\mu m$  for  $fCOx$ -MWNT and  $1.1\mu m$  for  $f$ -MWNT. Nanotubes treated for 24 hours decrease in length:  $0.7\mu m$  for  $fCNx$ -MWNT,  $0.6\mu m$  for  $fCOx$ -MWNT and  $0.5\mu m$  for  $f$ -MWNT. 200 $\mu l$  of nanotubes in solution were dropped on silicon substrates and were allowed to dry. All bar scales are  $2\mu m$ .

The first result of bacteria transformation is a visual characterization, and consist of counting colonies of MRS-Agar plates. The number of colonies provide important data regarding the transformation efficiency. Table 4.1 describes transformation rate of *B. longum* transformed with our technique. In contrast, table 4.2 summarizes the most important reports of *B. longum* transformation.



**Figure 4.4** Photograph of MRS-Agar plate with colonies of *B. longum*. The MRS-agar plate contains chloramphenicol, as a transformation marker.

**Table 4.1** Transformation rate of *B. longum* with three different transformation methods and CNTs.

Nanotube	Treatment	Efficiency (transformants per $\mu\text{g}$ of DNA)
FCNx-MWNT	Electroporation	$3 \times 10^3$
	Heath shock	$11 \times 10^6$
	Microwaves	$14 \times 10^6$
f-COx-MWNT	Electroporation	$17 \times 10^3$
	Heath shock	$22 \times 10^6$
	Microwaves	$22 \times 10^6$
FMWNT	Electroporation	$5 \times 10^3$
	Heath shock	$10 \times 10^6$
	Microwaves	$8 \times 10^6$
<b>Control</b>		
<i>B. longum</i> ATCC 15707	Electroporation	12
	Heath shock	0
	Microwaves	6

**Table 4.2** Transformation rate reported for three different groups, all were made by electroporation and used high voltages, with exception of LeBlanc,

Group	Bacteria	DNA	Treatment	Efficiency (transformants per $\mu\text{g}$ of DNA)
Mateuzzi et al	B. longum MB219	pNC7	Electroporation (12.5kV/cm-1)	$4.1 \times 10^2$
	B. longum MB260	pNC7	Electroporation (12.5kV/cm-1)	$9.3 \times 10^2$
LeBlanc et al.	B. longum 2577	pRM2	Electroporation (2 kV/cm-1)	$3.8 \times 10^2$
	B. longum U2	pDG7	Electroporation (12kV/cm-1)	$2.6 \times 10^3$
Argnani et al	B. longum Wiesby	pDG7	Electroporation (12kV/cm-1)	$7 \times 10^4$

The electroporation of Mateuzzi [11] and Argnani [13] were carried out using 12.5kV. LeBlanc [12] reported high efficiency when applying low voltages, but this sample preparation is more complex. We therefore propose three simple and efficient ways for achieving an efficient transformation.

PCR confirms that hIL-10 is integrated to the bacteria genome, the Agar-gel is shown in figure 4.5. The first band corresponds to the molecular size marker, each of the bands in this place corresponds to a different molecular size. The arrow indicates a molecular size of 500 base pairs (bp); note that the size of DNA synthesizer of protein hIL-10 is 490 bp

There are few reports regarding the interaction of bacteria and CNTs. Since bacteria are the most numerous organism over the planet, it is important to carry out interactions studies with nanosystems. However, most of the papers describe bactericidal properties of CNTs.

In this context, Liu et al. in 2007 [1] published the bactericidal properties of coated CNTs, and found a high rate of death bacteria, *Escherichia coli* and *Staphylococcus aureus*. In the same year Kang et al. [2] exposed SWNT to *E. coli* and found strong antimicrobial activity. Subsequently Brady-Esteves et al. [3] developed a filter based on SWNTs to remove viruses (MS2 bacteriophage, as virus model) and bacteria (*E. coli*) from water, and Srivastava et al. [4] built a filter based on SWNTs to retain *E. coli* and poliovirus.

In our knowledge there is only one report about bacterial transformation with CNTs. This report, by Rojas-Chapana et al [5], describes the behavior of *E. coli*

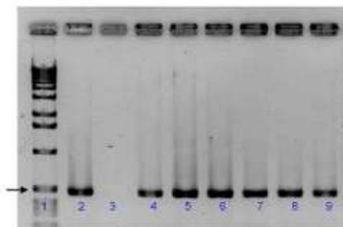


**Figure 4.5** PCR amplification of gene fragments cloned onto pLR-hII-10 plasmid. The arrow shows the 490 pb corresponding to a hII-10 gene amplified fragment. Lane 1, DNA ladder (Invitrogen, 10bp DNA Ladder); Lane 2, positive amplification control; lane 3, negative transformation control. Lanes 4-9 corresponds to different *Bifidobacterium longum* colonies transformed with pLR-hII.10 with different transformation methods (lane 4-5: electroporation, lanes 6-7: heat shock, lanes 8-9: microwave).

SEM Images were taken in order to understand how and which nanotubes have a better interaction with bacteria. Sample preparation may introduce some undesirable effects, thus making interpretation more difficult. Figure 4.6 shows some joined bacteria through a union-bridge and when this join breaks, a small CNT appears attached to the membrane. These protuberances may be produced by sample preparation caused by glutaraldehyde or osmium tetroxide. An alternative reason is that when bacteria finalizes its mitosis phase, it may exhibit

little protuberances on its "ex joined" parts; these protuberances may be confused with small CNTs.

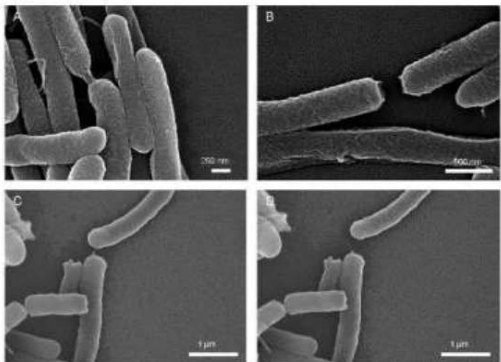


**Figure 4.6.** SEM images of bacteria with some protuberances (see arrows). This effect may be due to preparation. When we studied the samples, we observed a junction of two cells that starts to break while the electron beam hits the sample, two images were taken during this process, C and D, shows that the junction is not due to a CNT.

With SEM characterization we can clearly see if small diameter CNTs are adhered or pinned in to the membrane. Figure 4.7 shows small diameter  $f\text{CNx}$ -MWNTs (A and B) with great affinity for bacteria, meanwhile larger CNTs do not show that affinity due to its rigidity,  $f\text{COx}$ -MWNTs (C and D) shows a greater

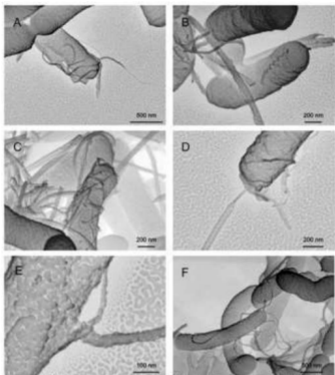


**Figure 4.7.** SEM images of *B. jugoslovanicus* treated with three different types of CNTs. A and B are *f*-CNTs-MWNTs; C and D are bacteria treated with *f*-CO<sub>2</sub>s-MWNTs and E and F are for bacteria treated with *f*-MWNTs. Images correspond to the negative of the originals.

attraction to bacteria. These data coincided with that contained in table 4.1 (MCH<sub>2</sub>-MPWNTs reaches the highest transformation rate), and figures E and F shows that these are not attracted by bacteria as does others CNTs.

By making an exhaustive search, we can find nanotubes piled to the membrane (see Figure 4.8). There is controversy about if CNTs can cross the bacteria membrane and stay inside (see Figure 4.8 B). STEM image helps to clarify this question. In all types of CNTs we observed this behavior.

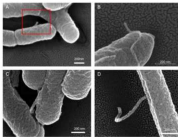


**Figure 4.8** STEM images of *B. lugeus* treated with CNTs, some CNTs seems to pile into membrane, is difficult to clarify if they are piled or just bends over cell membrane. Figures A, C and D are not clear if CNTs are inserted or they pass beneath the cell, image B is clearly that CNT is bended over cell membrane.



Larger diameter CNTs do not pin or penetrate the membrane, but bacteria seems to like to be with CNTs. Figure 4.9 displays large diameter CNTs with bacteria, somehow aligned and using them as templates for enhancing bacterial growth.

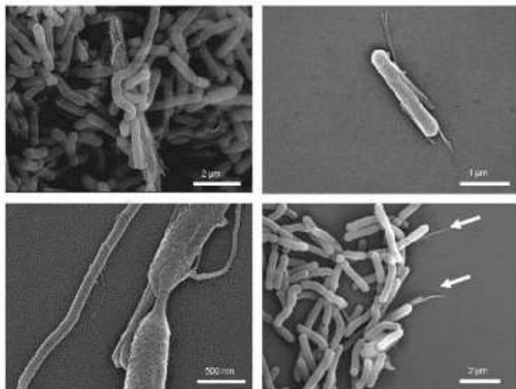


**Figure 4.9:** SEM images of large diameter CNTs with *B. longum*. Large diameter CNTs apparently does not cross the cell membrane. In A, bacteria are joined to a bundle of  $\beta$ -COx-MWNTs, which serves as templates. Some  $\beta$ -CNx-MWNTs tightly joined to bacteria, and they do not penetrate, diameter is 35nm and length 1-1.5 $\mu$ m, Bacteria length and diameter are 2.05  $\mu$ m and 24nm respectively; in C we find  $\beta$ -MWNT aligned with a bacteria, some CNTs with smaller diameter seems to be inserted into the membranes. Finally  $\beta$ -CNx-MWNTs follows the same direction of the bacteria axis, and this indicates that CNTs act as templates, see D.

By SEM characterization we noted a huge bacteria. It is noteworthy that the average length of bacteria is ca. 2  $\mu\text{m}$ , and the one observed in Figure 4.8, is 13 times longer (26  $\mu\text{m}$ ).

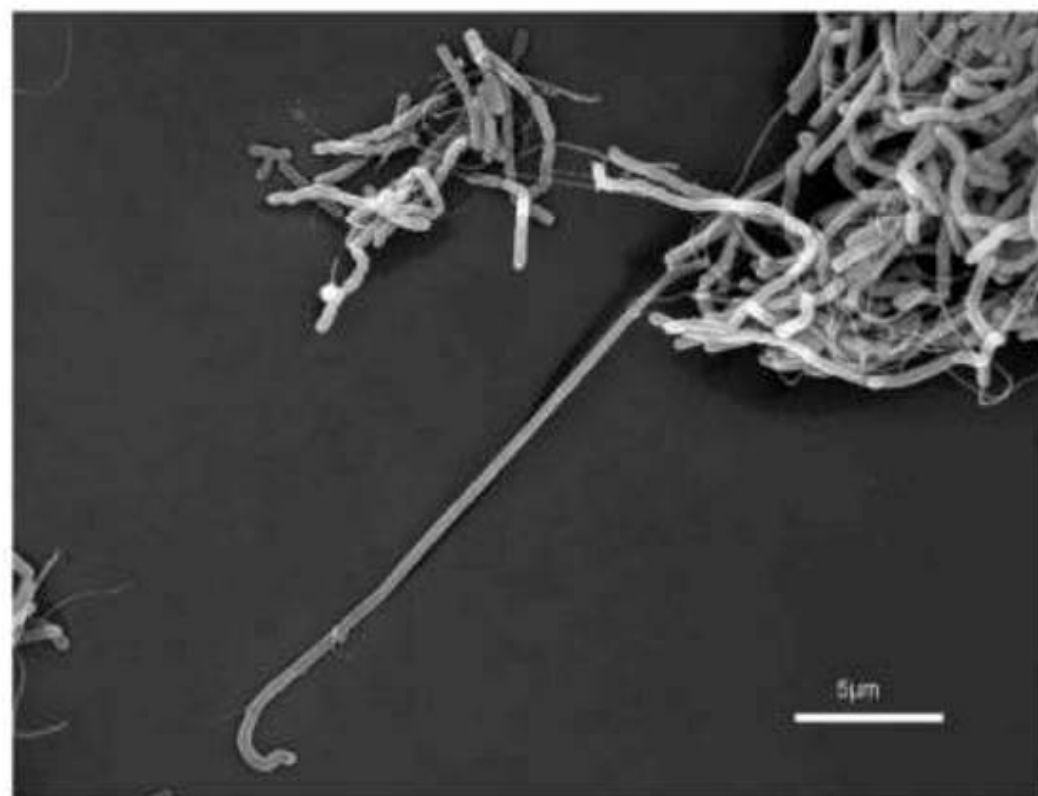


**Figure 4.10** SEM image of a huge bacteria, which could be grown from a nanotube which acts as a template.

Images like those depicted in Figure 4.10 were found several times, but we were also *f*MWNT crossing cell membrane Figure 4.11, Bacteria are not damaged and apparently tries to envelop it.

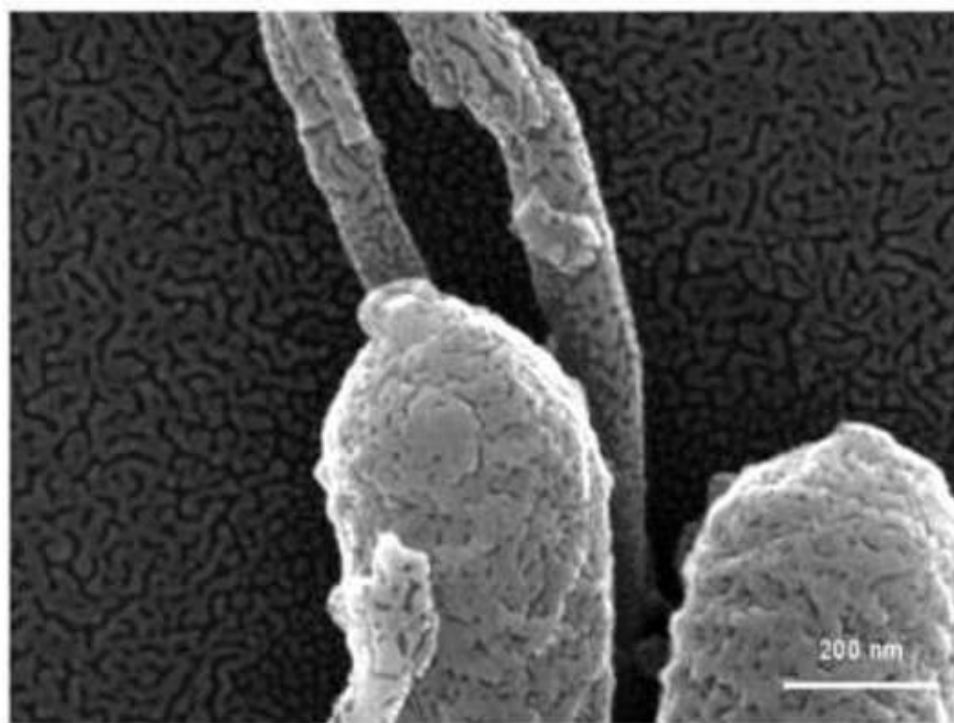


**Figure 4.11.** SEM image of a thick fCNTx-MWNT inserted in the bacteria. This type of images were not commonly observed.

In order to verify if CNTs attach or penetrate the cellular membrane, we used STEM characterization. With this technique we can visualize cross-sections of bacteria. The slices have an average thickness of 60nm. Figure 4.12 illustrates that large nanotubes attach to the cell membrane, but do not penetrate the cell. Dark high contrast regions correspond to iron particles encapsulated inside nanotubes.

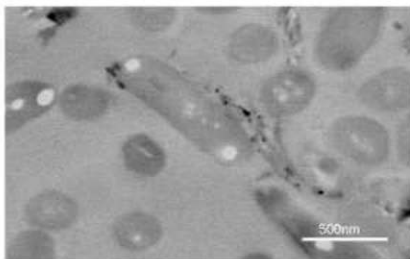


**Figure 4.12.** STEM image of *B. longus* and f/CNx MWNTs. Sample was fixed, dehydrated, stained and embedded in epoxy resin. It can be observed only two bacteria ordered transversally.

Figure 4.13 shows a possible sequence on how CNTs could penetrate the cell membrane. Possibly by opening or enabling channels by which genetic material goes into the bacterium.

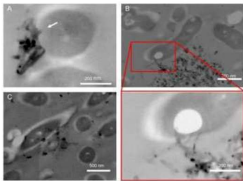


**Figure 4.13.** SEM images of  $\beta$ CNTs-MWNTs with *B. lagan*. In A the arrow indicates a nanotube ( $\beta$  ~31.3nm) possibly penetrating or anchoring into the membrane. In B a group of three nanotubes piercing the membrane is observed. Higher magnification reveals iron particles encapsulated inside CNTs. In C, small diameter CNTs ( $\beta$  ~21nm) appears crossing the cell membrane.

It is evident that CNTs enhance by two orders of magnitude the transformation rate of *B. lagan*. The exact process is still far from clear, but we believe that CNTs debilitate the membrane due to surface interactions occurring among functional groups present on the surface of the nanotubes and the cell membrane proteins, thus subjecting the cell to stress and facilitating the entrance of incoming of genetic material.

## References

- [1] Liu, T., Tang, H. Q., Cai X. M., Zhao J., Li D. J., Li R., Sun, X. L., A study on bactericidal properties of Ag coated carbon nanotubes, *Nanot. Instr. and Meth. in Phys. Res. B* (2007) 264 282-286.
- [2] Kang, S., Pinals, M., Pfeifferle, L. D., Elimelech M., Single-Walled Carbon Nanotubes Exhibit Strong Antimicrobial Activity, *Langmuir* (2007), 23, 8670-8673
- [3] Brady-Estevcz, A. S., Kang, S., Elimelech, M., A Single-Walled-Carbon-Nanotube Filter for Removal of Viral and Bacterial Pathogens, *Small* (2008), 4, No. 4, 481-484
- [4] Srivastava, A., Srivastava, O. N., Talapatra, S., Vajtai R., Ajayan P. M., *Nature Materials*, (2004) 3, 610-614
- [5] Rojas-Chapana, J., Troszczynska, J., Firkowska, I., Morszczek, C., Gicrsig, M., Multi-walled carbon nanotubes for plasmid delivery into *Escherichia coli* cells. *2005 Lab Chip*, (2005) 5, 536-539
- [6] Ishibashi, N., Yasuhira, T., Hayasawa, H., Bifidobacteria: their significance in human intestinal health, *Mal J Nutr* 3: 149-159, 1997
- [7] Yazawa, K., Fujimori, M., Amano, J., Kano, Y., Taniguchi, S., *Bifidobacterium longum* as a delivery system for cancer gene therapy: Selective localization and growth in hypoxic tumors, *Cancer Gene Therapy*, (2000) 7, 2, 269-274
- [8] Reddy, B. S., Rivenson, A., Inhibitory Effect of *Bifidobacterium longum* on Colon, Mammary, and Liver Carcinogenesis Induced by 2-Amino-3-methylimidazo[4,5-f]quinoline, a Food Mutagen, *Cancer Research* 53, 3914-3418, September.

- [9] Singh, J., Rivenson, A., Tomita M., Shinamura, S., Ishibashi N., Reddy, B. S., *Bifidobacterium longum*, a lactic acid-producing intestinal bacterium inhibits colon cancer and modulates the intermediate biomarkers of colon carcinogenesis, *Carcinogenesis* (1997) 18, 4, 833–841.
- [10] Fu, G. F., Li X., Hou, Y.-Y., Fan, T-R., Liu, W-H., Xu, G.-X., *Bifidobacterium longum* as an oral delivery system of endostatin for gene therapy on solid liver cancer, *Cancer Gene Therapy* (2005) 12, 133–140
- [11] Rossi, M., Brigidi, P., Mateuzzi, D., An efficient transformation system for *Bifidobacterium* spp. *Letter in Applied Microbiology* (1997), 24, 33-36
- [12] Missich, R., B. Sgsobati, and D. J. LeBlanc. 1994. Transformation of *Bifidobacterium longum* with pRM2, a constructed *Escherichia coli*-*B. longum* shuttle vector. *Plasmid* 32:208–211.
- [13] Argnani, A., Leer, R. J., van Luijk, N., Pouwels, P. H., (1996) A convenient and reproducible method to genetically transform bacteria of the genus *Bifidobacterium*. *Microbiology* 142:109–114
- [14] Reyes Escogido, M. L., De Leon Rodriguez, A., Barba de la Rosa, A. P., A novel binary expression vector for production of human IL-10 in *Escherichia coli* and *Bifidobacterium longum*, *Biotchnol Lett*, DOI 10.1007/s10529-007-9376-8
- [15] Dager, M., Ehrlich, S. D., (1974) Prolonged incubation in calcium chloride improves competence of *Escherichia coli* cells. *Gene* 6, 23–28.
- [16] Fregel, R., Rodriguez, V., Cabrera, V. M., Microwave improved *Escherichia coli* transformation, 2008, *Letters in Applied Microbiology* ISSN 0266-8254
- [17] Jiang, K., Pitan, A., Schadler, I. S., Ajayan, P. M., Siegel, R. W., Grobert, N., Mayne, M., Reyes-Reyes, Marisol, Terrones, H., Terrones, M. Selective

Attachment of Gold Nanoparticles to Nitrogen-Doped Carbon Nanotubes *Nano*

*Lett.* (2003) Vol. 3, No. 3, 275-277.



A photograph of a laboratory setup. On the left, a test tube is held in a white stand, containing a yellow-orange liquid. To the right, several petri dishes are arranged on a dark surface. In the foreground, a white paper is partially visible. The background is a grid pattern.

## Chapter 5:

Conclusions and Future work

## Conclusions

Nanotubes were synthesized successfully using the CVD process. The tubes we obtained are multiwalled carbon nanotubes and could be functionalized using an acid treatment in order to disperse the tubes in water or a medium for cell culture.

We were able to reproduce the results reported by different groups, observing that MWNT can penetrate human cell membranes. It is noteworthy that reports dealing with the interactions between nanostructures and bacteria are very scarce.

In this thesis we demonstrated that cells exhibit different behavior depending on the nanotube concentration, dispersion, time of interaction, and cell type. Therefore, for different cells not only cancer cells, the interaction is very different. In addition, when adding MWNTs into cell culture the cell apoptotic percentage increases. In fact, we can observe drastic changes in all the cell cycles.

In the same context, apparently it is possible to achieve some phase arrest due the interaction with CNTs, of course, it depends on nanotube type, concentration, time of interaction and cell type. We observe an increase in the apoptosis rate for almost all the cases. The  $f$ -CNTs-MWNTs exhibit the less apoptosis index in cancer cells, but in HEK cell it presents the lower apoptosis rate, this when the cell are treated for 24 hours.

In this work, we were also able to increase the *Bifidobacterium longum* transformation rate by two orders of magnitude, only by making a pre-mixing of DNA and MWCNTs in conjunction with traditional transformation techniques: electroporation, heat shock and microwave radiation. The efficient transformation of BL could have a large impact in novel oncology treatments.

Interactions with different MWNTs sizes were observed, small diameter MWNTs can usually penetrate into the bacteria membrane without trouble. Moreover, thick diameter CNTs seem to act as a guideline for bacteria growth. Only in few cases, thick diameter CNTs were found pinned into bacteria. Probably CNTs are able to form nanochannels or pores by which plasmid could pass.

The transformation rate becomes larger when short CNTs are used. This is due the presence of short nanotubes and because they are more flexible and have a greater contact with bacteria. Thicker nanotubes act as pins, and, in some cases, may perforate cell membrane, thus facilitating the plasmid to pass through.

## Future work

It may be necessary to verify the response of different functionalization process, in MWCNTs, such as the non covalent Functionalization. These treatments may result in unexpected results when interacting with biological systems.

A full characterization of CNTs using Scanning-Transmission X-Ray (STXR) microscopy. This characterization may provide us with a better idea of how the functionalization of carbon nanotubes takes place. The degree of functionalization for different times in acids appears to be an important factor when interacting with bio-systems.

The use of different sizes of nanotubes will provide us a better idea of nanotube toxicity. However other carbon nanostructures such as nano-cones, nano-horns, fullerenes, graphene or single walled carbon nanotubes need to be studied with human cells and bacteria.

We need to look up for the best conditions for bacteria transformation. There are a number of variables including nanotube length, nanotube diameter, degree of functionalization, time of interaction with bacteria before transformation treatment, concentration of nanotubes, parameters in electroshock apparatus, conditions in microwave, that appear to be very important in the process described in this thesis.

## Appendix A

### Cell Culture maintenance.

All material must be sterile, and follow all steps carefully.

To defrost cells follow the next steps:

1. Thaw the cells in a 37°C water bath, warm quickly and keep shaking
2. As soon as the cells thaw, pipette the cells into a tube with medium containing 20% serum.
3. Change the medium as soon as the cells are adherent (the next day) so that the DMSO is removed.

When the density cells are high it is necessary to remove some cells and relocate into a new cell culture plate. To accomplish this work follow the next steps:

1. Remove the medium carefully, the cells will keep adhered to the flask
2. Add trypsin, in order to detach the cell from the flask. Put in incubation for 5 minutes.
3. Add serum and fresh medium, serum will inhibit the trypsin effects.
4. Pipette the medium with cells into the necessary new flasks and store in incubator.

Some times is necessary to refresh the medium, in this case just omit the step 2.

## Appendix B

### Flow Cytometry, nucleus staining for FACS

#### III

Once finished the time of treatment with CNTs is necessary to know how the CNTs affect the cell cycle. The size of the nucleus tells us in which phase the cell is. Staining the nucleus with a proper fluorophore we can measure the size of the nucleus and indirectly know about the cell phase. The next steps explain how to stain the cell nucleus for flow cytometry characterization:

1. Harvest, wash the cells and adjust cell suspension to a concentration of  $1-5 \times 10^6$  cells/ml in ice cold PBS. Cells can be stained in any container for which you have an appropriate. In general, cells should be spun down hard enough that the supernatant fluid can be removed with little loss of cells, but not so hard that the cells are difficult to resuspend.
2. Add 0.1-10  $\mu\text{g/ml}$  of the primary labelled antibody. Propidium iodide is added at this point for dead cell exclusion.
3. Incubate for at least 30 min at room temperature or 4°C. This step will require optimization.
4. Wash the cells 3X by centrifugation at 400 g for 5 minutes and resuspend them in 500ul to 1ml of ice cold PBS.

Keep the cells in the dark on ice or at 4°C in a fridge until your scheduled time for analysis.

5. Analysis. For best results, analyze the cells on the flow cytometer as soon as possible.

[1] abcam. Direct Staining Protocol. [www.abcam.com/technical](http://www.abcam.com/technical)

## Appendix C

# Cell preparation for Scanning and Transmission Electron microscopy [2].

There are 6 steps for biological sample preparation for electron microscopy [1]:

- Fixation
- Dehydration
- Infiltration
- Embedment
- Sectioning
- Staining

### **Fixation:**

The most common way of fixation is through chemical fixatives. There are some basic factors that can affect fixation (pH, osmolality, temperature, length of fixation and the method of fixation). *Fixation must be uniform throughout the specimen.*

The final osmolality have different effects on the final appearance of the cells. Osmolality can be adjusted by several methods:

- adjusting non-electrolytes: sucrose, glucose, dextran or PVP
- adjusting electrolytes: NaCl, CaCl<sub>2</sub> (before adjusting pH)

The mammalian tissues have an ideal osmolality in the range of 500 to 700 mOsm. A commonly fixatives used are:

**Phosphate Buffer:** More physiological than other buffers, non toxic, stable in a wide range of temperatures. Cause some swelling and bind polyvalent cations.

**Glutaraldehyde:** small molecular size, its two aldehyde groups can crosslink compounds and act as a molecular bridge between macromolecules. Do not react with lipids. The temperature and the concentration are critical factors, (4°C and 1.5 – 4% is recommended)

**Osmium Tetroxide:** can be used as a liquid fixative or a vapor fixative. It has a low rate of penetration, because of this is used as a secondary fixative. Osmium serves as an electron stain. Its most useful ability is to fix lipids. An  $OsO_4$  is necessary if we want to preserve membranes and lipid containing bodies. Typically used at a concentration of 1-2% in buffer. It almost totally destroys antigenicity of reactive sites. Ruthenium tetroxide is sometimes used as a less expensive alternative.

There are basically four methods of fixation:

- Vascular perfusion
- Immersion
- Dripping in the surface
- Injection.



The only technique applicable for cell fixation is immersion; cryofixation is another common technique.

**Dehydration:**

The fixative must be removed. We can do it replacing the fixative with pure buffer in the same concentration and pH, two or three changes of buffer in a period of 10-20 min.

It is necessary to remove precipitated salts during buffer wash; the salt might affect the polymerization. Water removal is achieved bringing the sample through a graded series of ethanol or acetone.

After reaching an ethanol concentration of 100% we bring the sample in 100% propylene oxide (PO) twice, this is an optional step. The propylene oxide is used because most epoxy resins are more soluble in PO than in ethanol, but it has an inconvenience as the PO is extremely good extracting lipids, also PO can react with epoxy groups of the resin and inhibit polymerization.

Dehydration times should be kept at minimum 1 hour. Some resins tolerate small amounts of water and one can begin the infiltration process before the dehydration is complete. The use of a slow rotator is recommendable to keep the sample moving and always in contact with fluid.

**Embedding medium:**

The only purpose of embedding medium is to have a medium that permit cut thin slices, this medium must be non-reactive, must keep unchanged during

microscopy, attach the biological sample and it should be transparent to passage of electrons.

**Epoxy Resins:** the epoxy ring reacts with virtually any available hydrogen, epoxy resins need hardeners, these are groups of dicarboxylic acids or anhydrides (dodecyl succinic anhydride DDSA and/or nadic methyl anhydride NMA). Both components must be thoroughly mixed.

The ability to penetrate tissues of epoxy resins is reduced, to overcome this factor we can use a clearing agent, for epoxy resins PO is used between the last dehydration step and the beginning of infiltration.

There are another alternative embedding medium: durcupan, aquon, 10% of polystyrene in acetone, LR White and Lowicryl.

### **Sectioning:**

Conventional microtomes used for preparing light microscopic slides are inadequate for cutting sections of the required thickness for TEM. For this reason an ultramicrotome is employed (A ultramicrotome is an apparatus of very high degree of accuracy which allows cuts from 60 to 100 nm being useful in electronic microscopy).

It has an operation similar to the microtome. The mechanical advance is replaced by a thermal advance regulated by an electronic device, the steel knife is replaced by a knife of glass or of diamond and the operations are done under the control of a binocular magnifying glass. The cuts are collected on grids and not on blades[4].

There are some important points that could be a problem when slicing: the most common is improper resin polymerization, it could be attributed to a number of factors including incomplete dehydration and/or infiltration, uneven mixing resin, improper polymerization conditions, etc.

The largest dimension of any block face should not exceed 0.5mm and it should have a trapezoidal form, the bigger side goes in the bottom of the boat.

If the slide is up to 0.25um thick, for epoxy resins, it can be used in TEM operating at 100KV

#### **Staining of sections:**

The most commonly used stains in electron microscopy are made up of heavy metals salts.

**OsO<sub>4</sub>**: it reacts more rapidly with lipids than it does with proteins.

**Uranyl acetate (UA) & lead citrate (LC)**: UA reacts with phosphates and amino groups, while lead ions bind to negative charged molecules such as hydroxyl groups. UA have the ability to stain different cellular components.

The stain with UA can be applied before dehydration; it is applied to the specimen as a 0.5 – 4% aqueous solution after the initial fixatives. Then the specimen is dehydrated and infiltrated as normally done. The dehydration should not be long, the solvents can remove UA. This step helps with the contrast of membranous structures such mitochondria, golgi, ER, DNA and other fine filaments.

When the sample has been dried it can be stained on the grid, this step is done by floating the grid on a drop of 1 – 4% UA for 15min, then the grid is rinsed, dried and stained with LC or stored

The stained of the grids should be within 24 hours of having cut the sections. After the stain of UA is common to stain with LC, LC is very reactive with CO<sub>2</sub> its necessary an atmosphere without CO<sub>2</sub>. Sections are stained floating the grids on drops of LC for 3 -5min. After staining the sections are rinsing in NaOH 1M and then rinsen in dH<sub>2</sub>O.

[2] This is a resume of the text from Center of Ultrastructural Research  
<http://www.uga.edu/caur/>

[3] Hyatt, A. D. (1991) *Immunogold techniques, in electron microscopy in biology: a practical approach* (Harris, J. R., ed) IRI. Press, oxford.

[4] [www.wikipedia.com](http://www.wikipedia.com)

# Appendix D

## Bacteria Transformation

### **Competent *B. longum* preparation**

*Bifidobacterium longum* ATCC 15707 strain was grown anaerobically for 8 hours at 37°C in MRS medium supplemented with 0.05% w/v L-cystein (Sigma). The culture was diluted 1:25 in fresh MRS and incubated again for 3 hours approximately, until an OD<sub>600</sub> of 0.2-0.4. Once reached this OD the culture was centrifuged (Sorvall, Model Super T21) at 8000 rpm for 15 minutes, the sample was decanted and rinsed twice with 0.5 M sucrose at 4°C, the cellular package were resuspended in 1/320 volume from original culture in 0.5M sucrose buffer.

Slowly were mixed 1.5 µg of plasmid DNA with 1.5 µg of nanotubes in solution and incubated on ice for 5 minutes. Then, was added 80 µl of competent *B. longum* cells and incubated in ice for 5 minutes.

### **Electroporation**

The electroporation method was carried out with a BIX ECM 830 pulser apparatus at a capacitance of 25 µF, resistance of 100Ω, voltage of 2 kVcm<sup>-1</sup> with a pulse of 2.1 miliseconds, according to Reyes-Escogido et al. (2007). Cells were immediately recovered in 200 µl of MRS medium and incubated for 3 hours at 37 Celcius degrees, subsequently the cells were diluted 1:1000000 and inoculated in the same medium agar plates containing

chloramphenicol at  $10 \mu\text{g ml}^{-2}$  as selection marker for transformants cells. Plates were incubated for 3-5 days at  $37^{\circ}\text{C}$ , under anaerobic conditions.

### **Heat shock**

For the heat-shock method, the cells were incubated on ice for 10 minutes, changed to a water bath at  $42^{\circ}\text{C}$  for 1 minutes and immediately changed the tube to ice for another 15 minutes. Cells were recovered with  $200\mu\text{l}$  of MRS medium and incubated for 3 hours at  $37^{\circ}\text{C}$ , subsequently the cells were diluted 1:1 000 000 and inoculated in medium agar plates containing  $10\mu\text{g ml}^{-1}$  chloramphenicol and were incubated for 3-5 days at  $37^{\circ}\text{C}$ , under anaerobic conditions.

### **Microwave**

For microwave transformation the potency of the machine was set at 115 watts and the time of treatment was 2 minutes, according with Cabrera et al. (2007) [5] and immediately were recovered in  $200 \mu\text{l}$  of MRS medium, plating and incubating were made in the same way as previous transformations.

A control experiment was performed using only traditional transformation process without nanotubes, in order to compare proposed treatments.

[5] A.A. Chvedova, V. Castranova, E.R., Kisin, D., Schwegler-Berry, A.R., Murray, V.Z., Gandelsman, a., Maynard, P. Baron. *J. Toxicol. Environ. Health Part A* (2003) 66, 1909-1926.

## Appendix E

### MRS Medium preparation [6]

#### Composition:

Ingredients	Grams/Liter
Peptone	10.0
Meat extract	5.0
Yeast extract	5.0
D(+)-Glucose (Dextrose)	20.0
Dipotassium hydrogen phosphate	2.0
Diammonium hydrogen citrate	2.0
Sodium acetate	5.0
Magnesium sulfate	0.1
Manganous sulfate	0.05
* Agar	12.0

Final pH 6.5 +/- 0.2 at 37°C

Store prepared medium below 8°C, protected from direct light. Store dehydrated powder, in a dry place, in tightly-sealed containers at 2-25°C.

Cystin is sterilized by filtration and added after the medium is sterilized in autoclave. 0.05 grams per liter were used.

\* Agar is added only for MRS agar plates, for liquid bacteria culture agar is omitted.

#### Directions:

Dissolve 61 g in 1 liter of distilled water and add 1 ml Tween 80 (Fluka No. 93780). Autoclave at 121°C for 15 minutes.

#### **Principle and Interpretation:**

The MRS medium formulation was developed by de Man, Rogosa and Sharpe to replace the tomato juice medium and the meat extract tomato juice medium. MRS is a medium supporting good growth of lactobacilli in general, even those strains which have shown poor growth in existing medium, like strains of *L. brevis* and *L. fermenti*. The MRS culture medium contain polysorbate (Tween 80), acetate, magnesium and manganese which are known to act as special growth factors for lactobacilli as well as a rich nutrient base. As these medium show a very low degree of selectivity, *Pediococcus* and *Leuconostoc* species as well as other secondary bacteria may grow on them. Most of the accompanying microflora can be inhibited by thallium acetate (Fluka 88204), sorbic acid (Fluka 85510), acetic acid (Fluka 45740), sodium nitrite (Fluka 71759), cycloheximide (Fluka 01810) and polymyxin (Fluka 81334). These substances can be used at varying concentrations and combinations, but inevitably a compromise has to be reached between selectivity and productivity of the organism sought.

[6] J. C. de Man, M. Rogosa and M. Elisabeth Sharpe, *Appl. Bact.* (1960) 23, 130-135.